Polymeric nanomaterial strategies to encapsulate and deliver biological drugs: points to consider between methods

Author

Chen, Xiangxun, Wu, Yuao, Dau, Van Thanh, Nguyen, Nam-Trung, Ta, Hang Thu

Published

2023

Journal Title

Biomaterials Science

Version

Accepted Manuscript (AM)

DOI

10.1039/d2bm01594c

Rights statement

Polymeric nanomaterial strategies to encapsulate and deliver biological drugs: Points to consider between methods

Xiangxun Chen[1], Yuao Wu[1], Van T. Dau[2], Nam-Trung Nguyen[1], and Hang Thu Ta[1, 3, *]

[1] Queensland Micro-Nanotechnology Centre, Griffith University, Nathan, Queensland 4111, Australia

[2] School of Engineering and Built Environment, Griffith University, Brisbane, Queensland 4215, Australia

[3] Bioscience Discipline, School of Environment and Science, Griffith University, Nathan, Queensland 4111, Australia

*Correspondence: Hang Thu Ta (h.ta@griffith.edu.au)

Corresponding author:

Hang Thu Ta, BEng, MSc, PhD

Associate Professor, School of Environment and Science and Queensland Micro- and Nanotechnology, Griffith University, Nathan Campus, Brisbane QLD 4111, Australia

Honorary Associate Professor, Australian Institute for Bioengineering and Nanotechnology, University of Queensland, St Lucia, Brisbane QLD 4067, Australia

Office: +61 (7) 3735 5384

Email: h.ta@griffith.edu.au

Website: https://hangta.group/

https://experts.griffith.edu.au/27034-hang-ta

Abstract

Biological drugs (BDs) play an increasingly irreplaceable role in treating various diseases such as cancer, cardiovascular, and neurodegenerative diseases. The market share of BDs is increasingly promising. However, the effectiveness of BDs is currently limited due to challenges in efficient administration, delivery, and issues with stability and degradation. Thus, the field is using nanotechnology to overcome the limitation. Specifically, polymeric nanomaterials are common BD's carriers due to their biocompatibility and ease of synthesis. Different strategies are available for BDs transportation, but the use of core-shell encapsulation is preferable for BDs.

This review discusses recent articles on manufacturing methods for encapsulating BDs in polymeric materials, including emulsification, nanoprecipitation, self-encapsulation and coaxial electrospraying. The advantages and disadvantages of each method are analysed and discussed. We also explore the impact of critical synthesis parameters on BDs activity, such as sonication in emulsification. Lastly, we provide a vision of future challenges and perspectives for scale-up production and clinical translation.

Keywords: Polymeric nanoparticles, emulsion, nanoprecipitation, nanomixer, self-assembly, coaxial electrospraying

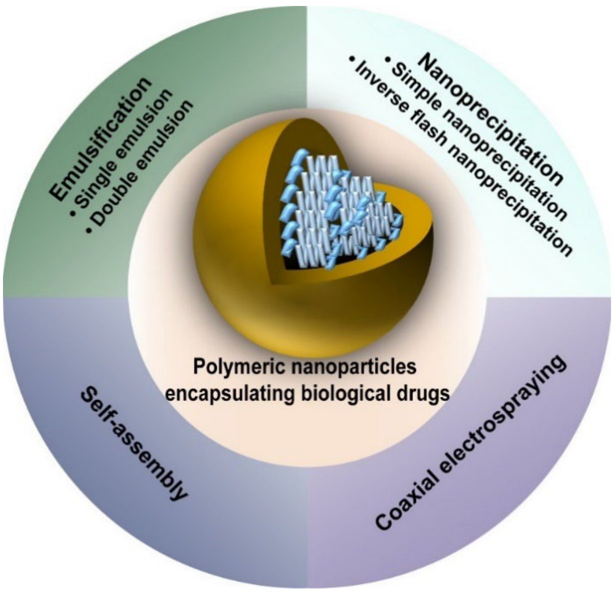

Graphical abstract: Different techniques developed for encapsulation of biological drug within polymeric nanoparticles

1. Introduction

The development of new therapeutic agents expands the range of available biological drugs (BD) for treating diseases or relieving relevant symptoms. BD is a group of medicines originating from living organisms with complex structures [1, 2]. Generally, BDs involve protein or enzyme-based therapeutics [3]. BD offers advantages over low molecular weight drugs as it can target more precisely with high potency, resulting in reduced intrinsic toxicity [1, 4]. Thus, BD is widely used for life-threatening diseases such as cancer, cardiovascular diseases, and other chronic diseases [5-7]. Since peptide-based insulin as the first BD was approved by the U.S. Food and Drug Administration (FDA) in 1982 to treat diabetes, the FDA has approved 621 BDs up to 2021 [8, 9]. In 2020, these BDs contributed to a US$253 billion pharmaceutical market and were forecasted to double in 2025 [10]. However, due to its nature, BD has disadvantages such as poor solubility, permeability, and bioavailability in oral delivery [11-13]. Moreover, for intravenous administration, BD accumulation in the bloodstream may induce a secondary off-target effect that could be lethal. For instance, a high administration rate of tPA (the only approved treatment option for stroke) may lead to tPA accumulation in different organs to cause haemorrhages such as the intracranial haemorrhage in hyperglycaemia and diabetes patients [14, 15]. Therefore, there is a need to find a solution to overcome these challenges to make full use of BD, which is beneficial to a broader population [16].

Nanoparticles (NPs) attract attention from the research community because of its wide range of applications, including diagnosis, analysis, imaging, and tissue engineering [17]. Moreover, NPs can act as carriers to deliver therapeutic agents [18]. The small size of NPs favours the permeability through different membranes and blood-brain barrier for a higher efficiency which has massively enhanced the therapeutic utility of the agents [19]. Additionally, applying appropriate targeting and releasing strategies can further improve the precision also the uptake rate of the original BD [20].

In terms of availability for use, FDA has approved over 20 NPs for clinical use, mainly inorganic NPs, liposomes, and polymeric NPs [19]. Inorganic NPs such as iron, silica and gold can be precisely synthesised into nanospheres, nanobundles and nanoshells to carry BD [21]. Inorganic NPs such as ^{111}In superparamagnetic iron oxide NPs can be employed as theranostic materials due to their unique radioactive and magnetic properties [22-38]. However, the biodistribution and cytotoxicity of inorganic particles are not fully investigated [39-41]. Moreover, the solubility of inorganic NPs is relatively low [42]. Therefore, it is challenging to translate inorganic delivery systems into clinical use, especially when heavy metals are employed as a part of the carrier.

Liposome is made up of phospholipids, which mainly form a spherical structure. This spherical structure can be multilayered and carry hydrophilic, hydrophobic, or even lipophilic drugs [43]. Since the FDA approved the first nano liposomal drugs in 1995, many studies have been devoted to the use of liposomes in disease treatment [44]. However, the drug encapsulation efficiency (EE) using liposomes as a delivery system is relatively low [45]. Besides, liposome carriers are mainly absorbed by the spleen and kidneys and release the drug in these organs [46]. This undoubtedly limited BD nano delivery to some extent. Since inorganic and liposome have certain disadvantages, other materials should be considered for the transportation and delivery of BDs.

Polymers are one of the most popular materials currently used for drug-loading nano-systems. Polymeric materials can be divided into non-biodegradable and biodegradable polymers [47]. Non-biodegradable nanopolymers such as acrylic polymers are generally used for local injection of antibodies or implant-bone components [47]. But their low biocompatibility and toxicity can lead to irreversible health complications [47]. Consequently, scientists focus more on developing biodegradable polymers such as polylactic acid (PLA) and poly lactic-co-glycolic acid (PLGA) to deliver drugs. Biodegradable polymeric materials do not produce harmful and non-biocompatible by-products upon degradation and therefore are generally not accumulated in major organs to produce cytotoxicity effects [48]. They can also be combined with inorganic NPs for therapeutic and diagnostic purposes [49, 50]. Degradable polymers have been explored as candidates for the delivery of targeted BD.

Methods to incorporate BDs to the nanoparticles include adsorption, conjugation and encapsulation [51]. Adsorption is a method that does not involve the formation of chemical bonds or the alteration of polymers, relying on van der Waals forces, electrostatic forces and hydrophobic interactions to anchor the BD to the relevant areas containing the lipophilic components of the polymer [52]. These interactions, such as van der Waals forces, may aggregate and impact the colloidal stability, thus not supporting the stable transportation of BD to the target [53, 54]. This may cause a reduction in the BD efficiency. The exposed BD structure may also be altered by temperature and acidity change, thus limiting the usefulness of this method [55].

Conjugation is generally achieved by forming a covalent bond between the functional groups of BD and the polymer [56]. In this case, BD is exposed at the surface of the nanoparticles to facilitate targeting activity. Although conjugation may not impact chemical drugs, it may lead to BD denature and thus reduce BD efficacy [57-59]. Specifically, BD cannot be freely released to the target sites, and this binding may impact the conformational change of BD to bind to the target [60]. It would be helpful to retain BD activity while improving targeting efficacy.

Encapsulation is considered a as more suitable method for BDs transportation. BD can be encapsulated into polymeric materials without the involvement of covalent bonds to retain its activity [61]. Encapsulated BD can also be protected from body environment, pH, ions and enzymes. BD encapsulation combined with targeting strategies and stimuli-responsive strategies (e.g. pH or temperature) can enhance the use and efficacy of BD [62].

Each nanoparticle synthesis method offers its unique EE and results in a unique final product [63]. Common methods are emulsification, nanoprecipitation, self-assembly, and electrospraying [64-66]. Yet, the advantages and disadvantages of these methods have not been well documented. Therefore, this paper comprehensively reviews and compares methods to encapsulate BDs such as proteins, enzymes, plasmid deoxyribonucleic acid (DNA) and ribonucleic acid (RNA), offering better insights and knowledge toward improved nano delivery systems for BDs. The advantages and disadvantages of each method are analysed and discussed. We also explore the impact of critical synthesis parameters on BDs activity, such as sonication in emulsification. Lastly, we provide a vision of future challenges and perspectives for scale-up production and clinical translation.

2. Emulsification

Emulsification is the process of dispersing two or more immiscible liquids to form a semi-stable mixture. The emulsification method allows one phase of the liquids to be dispersed in tiny droplets in another phase to create a non-homogeneous emulsion system. Nano encapsulation using emulsion consists of a mixture of organic or oil phase and aqueous phase [67]. Depending on the continuous phase and the dispersed phase, they are divided into (1) oil-in-water emulsions, where the continuous phase is oil, and the dispersed phase is an aqueous solution; and (2) water-in-oil emulsions, where the continuous phase is an aqueous solution and the dispersed phase is oil [67]. Emulsification is generally classified into single emulsion and double emulsion for BD encapsulation.

2.1. Single emulsion

Single emulsion is one of the most frequently utilised methods for encapsulating BDss [68]. **Table 1** summarizes single emulsion studies for BD encapsulation in the last 5 years. Usually, this method utilises an aqueous solution of BDs followed by the addition of an amphiphilic polymer or a polymer with a stabiliser dispersed in the organic phase by homogenising techniques such as stirring or sonication. The help of an amphiphilic polymer or stabiliser allows the polymer to encapsulate protein. The particles solution from the previous step is processed by solvent evaporation to obtain the final NPs (**Figure 1**).

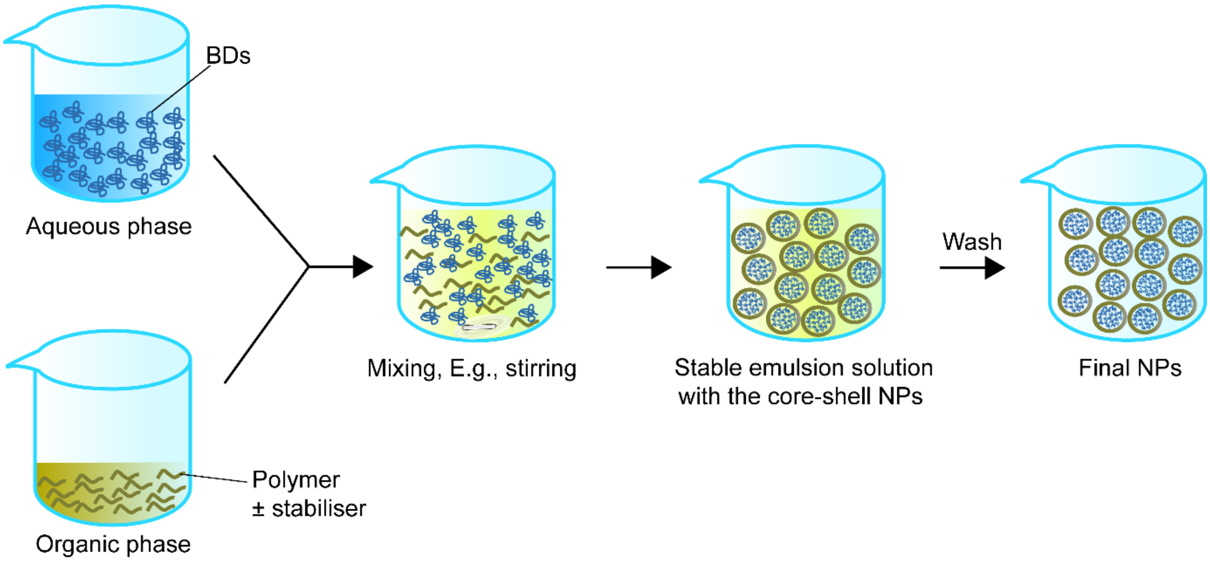

Figure 1. Schematic representation of single emulsion to synthesise core-shell nanoparticles.

Zamanlu et al. [69] demonstrated a single emulsion encapsulating protein with smaller particle sizes. Pegylated PLGA (PEG-PLGA) was employed to encapsulate tPA using single emulsion solvent diffusion/evaporation method. The size of the NPs was in the range of 200 – 300nm. The PEGylated PLGA-tPA NPs were 24.93 nm larger, and the EE was 4.83% higher than the PLGA-tPA group (89.85 ± 9.71%). Also, the loading capacity (LC) of the PEGylated PLGA-tPA NPs was higher than the PLGA-tPA group (3.60 ± 0.01% VS. 1.99 ± 0.01%). The cell viability and thrombolytic activity of the PEGlyated PLGA shell group were also higher than the PLGA only group. However, the study did not provide the *in vitro* release profiles for PEGylated-PLGA-tPA group, PLGA-tPA group and tPA only group. The information about how NPs with different structures perform in a prolonged period is thus limited. Furthermore, Dölen et al. [70] used a single emulsion with sonication for 2 minutes and 2.5% PVA as a surfactant. This study fabricated a New York esophageal squamous cell carcinoma 1 (NY-ESO-1) peptides mix-loaded PLGA NP of 227 ± 61 nm (PLGA 10 mg/mL, α-GalCer analog IMM60 at 50 µg/mL, and three immunogenic cancer germline antigen, NY-ESO-1 mix at 0.33mg/mL). The LC and EE were not reported. Similar levels of the immune response activated by the encapsulated IMM60, and NY-ESO-1 were found in vitro and in vivo, which was higher than the response from free IMM60 and peptide. The use of this NP has moved to phase I clinical trial for safety and tolerability assessment in humans (NCT04751786) [71]. Notably, the organic solvent used in this study during the preparation was dichloromethane and dimethyl sulfoxide (DMSO), but the reactivity of the peptides mix was not impacted.

NPs synthesised by single emulsion can also be employed for oral administration of BDs. Feng et al. [72] used methoxy polyethylene glycol (mPEG)-poly (β-amino ester) [PAE] to encapsulate bevacizumab (BVZ) with a single emulsion solvent evaporation method. The NPs size was 132.60 ± 0.058 nm, with an EE of 85.50 ± 0.33% and a LC of 0.54 ± 0.01%. They also used single emulsion to prepare a docetaxel-loaded Carboxymethyl chitosan (CMC)-PLGA NP. The two NPs were physically mixed to form a binary mixture at 132.60 ± 0.058 nm for dual anti-cancer treatments. Compared to the free drug groups in mice, the NPs mixture group had a higher absorption rate across the small intestine and a higher cytotoxic effect in non-small cell lung cancer cells. Moreover, the NPs mixture group had a higher plasma concentration than the free drug group (7.85 µg/ml at 50 min VS. 148.24 ng/ml at 50 min).

The NPs in these studies had a high EE but LC was lower than 10%. The low LC indicates that the BD cores formed in the core-shell NP structure are small and that the polymer shell makes up the bulk of the NPs. The low LC of hydrophilic BDs and the difficulty to scale up have prevented this method from being widely used. Knowing these drawbacks, a modified emulsion method, double emulsion was used to focus on core-shell encapsulation [73].

Table 1. Summary single emulsion studies for BD encapsulation in the last 5 years.

Encapsulated compounds	**Polymer**	**Surfactant or second polymer(s)**	**Applications**	**Size**	**Encapsulation efficiency, %**	**Loading capacity, %**	**References**
Proteins isolated from *L.panamensis.* - Soluble LpanUA.27.1860 - Insoluble LpanUA.22.1260	PLGA	PVA	Vaccine	LpanUA.27.1860: 36.56 µm at 750 µg/ml LpanUA.22.1260: 44.97 µm at 750 µg/ml	LpanUA.22.1260: 94.66 ± 4.86 LpanUA.27.1860: 89.03 ± 4.91	/	[74]
tPA	PEG-PLGA	/	Thrombolysis	276.20 ± 27.58nm	94.78 ± 3.09	3.60 ± 0.01	[69]
BVZ	mPEG-PAE for BVZ	/	Anti-cancer	BVZ loaded: 82.07 ± 0.19nm Binary mixture: 132.60 ± 0.058 nm	BVZ loaded: 85.50 ± 0.33	BVZ loaded: 0.54 ± 0.01	[72]
NY-ESO-1 and IMM60	PLGA	PVA	Anti-cancer	At PLGA 10 mg/mL and peptides	/	/	[70]

				content of NPs of 11.4, 13.4, and 11.5 μg/mg: 227 ± 61 nm			

2.2. Double emulsion

In the early 1980s, Matsumoto et al. [75] introduced the concept of double emulsion. The double emulsion technique is an expanded version of a single emulsion with two common types, water-oil-water and oil-water-oil. For instance, in the water-oil-water type, the primary emulsion solution contains an aqueous phase with BD and an organic phase with the polymer or stabiliser. Then the primary emulsion solution is added to a second aqueous phase. Sonication helps the secondary emulsion solution for stable core-shell structure NPs. Finally, the NPs in the secondary emulsion solution can be collected via solvent evaporation (**Figure 2**). **Table 2** summarizes double emulsion studies for BD encapsulation in the last 5 years.

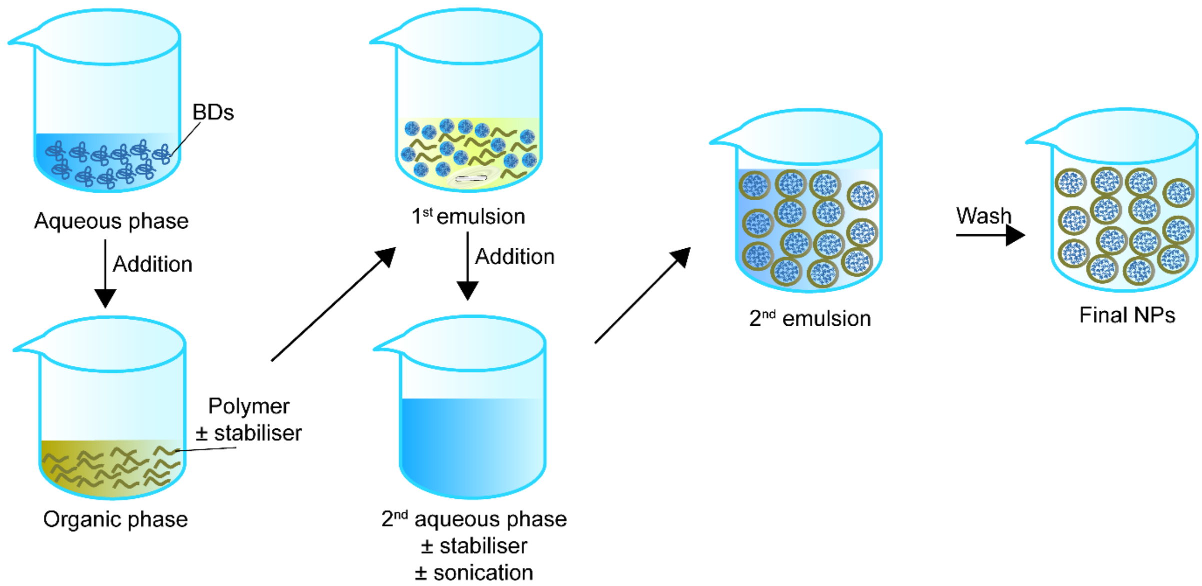

Figure 2. Schematic representation of double emulsion to synthesise core-shell nanoparticles.

2.2.1. Sonication in double emulsion

Most recent studies used the double emulsion method with sonication to achieve better results. In theory, sonication generates heat that may affect the properties and activity of the encapsulated BDs [76,77]. However, recent studies did not support this view. For instance, Steiert et al. [78] reported a polyethylene glycol-modified lysozyme to encapsulate naïve lysosome size 180-220 nm to treat gram-positive *Micrococcus luteus (M. luteus)*. Sonication was an aid in forming stable emulsion to load the lysosome. Boushra et al. [79] also supported this point. They found that one minute of 50% amplitude sonication under an ice bath for the double emulsion retains insulin stability. The study employed a hydrophilic polymer PEG_{6000} to increase the entrapment of protein insulin in the internal aqueous phase and reduce its tendency to leak to the external aqueous phase. The aqueous mixture of PEG and insulin was added to the organic phase containing PLGA and trimyristin lipid to form a w/o emulsion with insulin and 2 polymers. The w/o phase was then added to an aqueous phase to from w/o/w double emulsion. The size of the insulin/PEG loaded PLGA-trimyristin NPs was 85 nm smaller than the insulin-loaded trimyristin NPs, while EE was 30% higher than the insulin-loaded trimyristin NPs.

Furthermore, sonication in double emulsion does not influence the activity of small size BDs. For example, Priwitaningrum et al. [80] prepared a second mitochondria-derived activator of caspase (Smac) loaded polymeric NPs with an average diameter of 197 nm for anti-tumour purposes. The first emulsion solution was formed by 30 seconds of sonication at 10 % amplitude with the presence of Smac peptide saline solution, $mPEG_{2000}$-PLGA and PLGA in an ice bath. PVA was added to the solution, followed by 1-minute sonication at 10% amplitude to stabilise the NPs. The Smac NPs achieved an EE of 48% and 2.4% LC. Sonication did not impact the *in vitro* and *in vivo*. The *in vitro* results indicated that after 10% amplitude sonication, the NPs were still able to induce triple-negative 4T1 mouse breast tumour cells apoptosis rapidly. Besides, the NPs expressed a synergistic anticancer effect with doxorubicin *in vivo.*

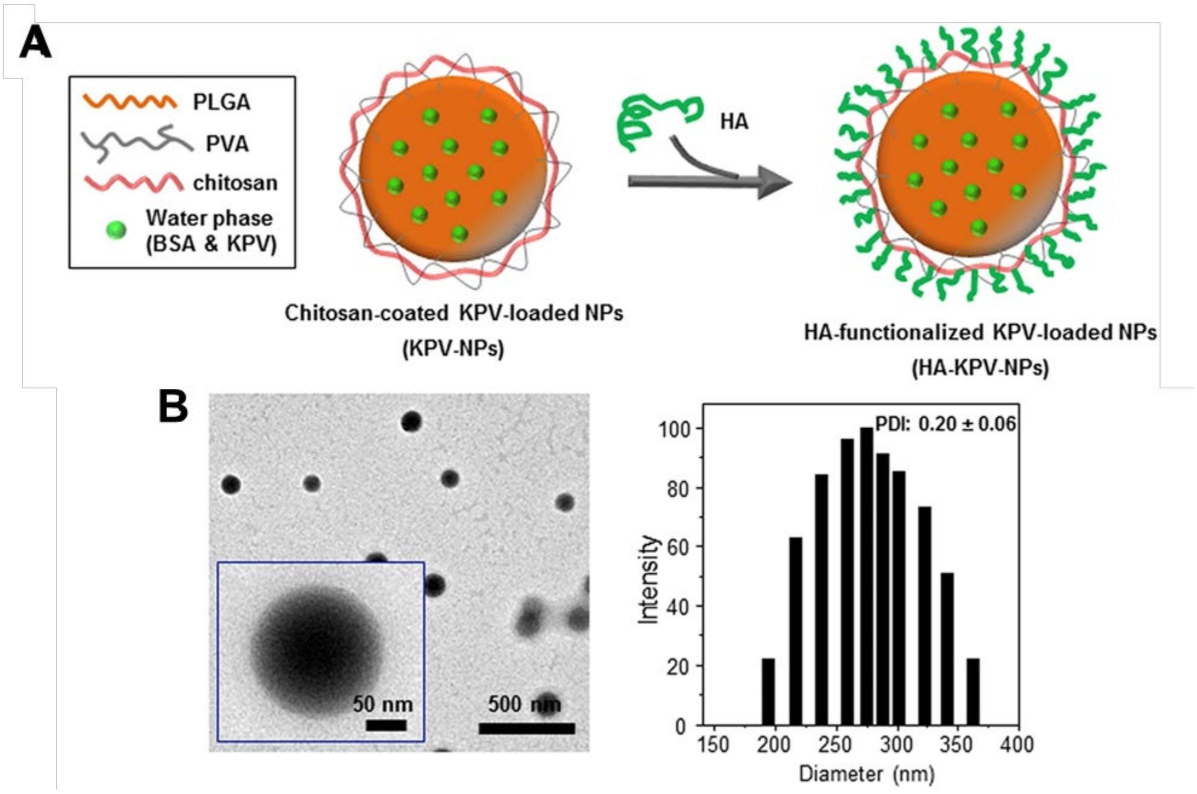

Figure 3. Preparation and Characterization of KPV-Loaded Polymeric NPs. (A) Schematic illustration of the fabrication process of HA-KPV-NPs. **(B)** Representative TEM images and the corresponding size distribution of HA-KPV-NPs**.** Reprinted from Ref. [81],

copyright (2017), with permission from Cell Press.

Similarly, Xiao et al. [81] utilised a PLGA-PVA-chitosan polymer with hyaluronic acid (HA) functionalised coating to deliver lysine-proline-valine (KPV) using a double emulsion with sonication for ulcerative colitis (UC) treatment. KVP was dropwise added to the PLGA containing organic phase to form the primary emulsion solution for synthesis. Sonication was applied to the primary emulsion solution 10 seconds for six times with PVA and depolymerised chitosan. With an average size of 272.3 nm, the NPs remained intact after oral administration across the stomach and aggregated towards the wound of colonic epithelial cells in a UC mouse model (**Figure 3**). Even though the authors previously proved that the therapeutic efficacy of KPV in the non-functionalised NPs was 12000-fold lower than the free KPV concentration [82], in this study, they did not directly compare the therapeutic efficacy of the non-functionalised NPs to the functionalised NPs. Xiao et al. [81] only demonstrated that the tissue uptakes of the functionalised NPs were higher than not non-functionalised NPs at 4 hours and 18 hours.

Minooei et al. [83] demonstrated that two times sonication (no amplitude showed) in double emulsion did not reduce the effect of an oxidation-resistant variant of griffithsin, an algae-derived antiviral BD for defecting human immunodeficiency virus-1 (HIV-1) infection *in vitro*. PVA was presence in both primary and secondary emulsion solutions as a stabiliser. The griffithsin variant was encapsulated in a PLGA core with a size of 98.5 ± 37.2 nm, accompanied by a 48.9 ± 12.7 % EE and 48.9 ± 12.7 μg/mg LC. Also, the half-maximal inhibitory concentration (IC50) of the griffithsin variant NP was 4.09-fold lower than its free form (1.1 nM vs 4.5 nM), which indicated that griffithsin variant NP prevented HIV-1 infection better than the free griffithsin *in vitro.*

Double emulsion with sonication was able to load small interfering ribonucleic acid (SiRNA) [84]. In the study they used a PEG-PLA with an amphiphilic dendrimer, G0-C14 and paclitaxel as the shell to load siRNA, for matrix metalloproteinase-rich tumours treatment. A 30 seconds 80 w sonication for the primary emulsion and 2 minutes 100 w sonication for the secondary emulsion did not impact the binding activity and stability of the siRNA. Later, Zhang et al. [85] synthesised a 90 nm NP by double emulsion with ice-bathed about 12% amplitude ultrasonication to encapsulate siRNA with folic acid (FA)-modified PLGA-thioketal (TK)-PEG. The NPs with the siRNA had lower tumour volume from day 1 to day 16 than the free siRNA group and the non-specific siRNA group. It inhibits the translation of the corresponding protein by binding to the messenger RNA (mRNA) of the target gene.

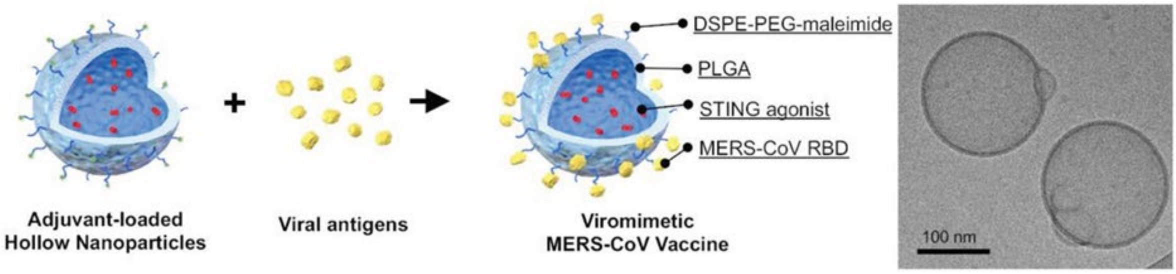

Figure 4. Characterization of adjuvant-loaded viromimetic nanoparticles. A schematic showing the preparation of viromimetic nanoparticle vaccine. Hollow PLGA nanoparticles with encapsulated adjuvant and surface maleimide linkers were prepared using a double emulsion technique. Recombinant viral antigens were then conjugated to the surface of nanoparticles via thiol-maleimide linkage. Cryo-electron microscopy of cdGMP-loaded hollow nanoparticle. Reprinted from Ref. [86], copyright (2019), with permission from Wiley.

There are a few studies successfully encapsulating small BDs using sonication in double emulsion. For example, Lin and his group loaded cyclic diguanylate monophosphate (cdGMP, 0.69kDa) within hollow PLGA NPs (114 nm) for a Middle East Respiratory Syndrome Coronavirus vaccine [86]. A 40 % amplitude (1 minute) for primary emulsion then 30 % amplitude (2 minutes) for the secondary emulsion for did not impact the activity of cdGMP and able to achieve 48% EE (**Figure 4**). Moreover, Ural et al. [87] did a study using 40% amplitude sonication twice during double emulsion to load vancomycin (1.45kDa) in PLA-PLGA shell. The first sonication was done for 15 s to the primary emulsion solution containing vancomycin and PLA-PLGA solution. Then the solution was added to sodium chloride solution with 0.5% w/v PVA to form the secondary emulsion. The secondary emulsion solution was sonicated at the same amplitude for 30 s. The optimised particles had a size of 319 nm, 50 ± 7% EE and 23 ± 3% LC. However, this study did not explore the *in vitro and vivo* therapeutic utility of the NPs. These results suggest that use of sonication can be translated to small BDs encapsulation.

Liao et al. [88] studied the size and activity of enzyme-loaded polymeric NPs prepared in either 1 wt% cholic/deoxycholic acid (CHA) sodium salt or 1 wt% PVA surfactants under different sonication conditions for double emulsion. The PEG-PLGA coated catalase NPs with CHA and sonicated for 15, 30, and 60 seconds were smaller than those with PVA prepared under the same settings. Their size at 15 s to 30 s and 60s were similar for CHA as well as PVA groups (~80 nm for CHA and ~120 nm for PVA at 15, 30 and 60 seconds of sonication). For the catalase activity, the group sonicated for 30 seconds had the highest catalase activity of about 45 units/ml and 80 units/ml for CHA and PVA, respectively. Further sonication, such as 60 seconds, reduced catalase activity by 30 units/ml compared to those from 30 seconds (for both CHA and PVA groups). Sonication of less than 30 seconds also reduced the catalase activity. The 15 seconds sonication results for the CHA and PVA groups were about 10 units/ml and 5 units/ml, respectively, lower than its 60 seconds sonication results. Surprisingly, sonication for one second did not preserve the catalase activity for both groups but resulted in the least activity (~5 units/ml and ~40 units/ml for CHA and PVA, respectively).

Although the sonication time of some studies mentioned above was higher than the range reported by Liao et al. [88], the encapsulated BDs, regardless of their sizes, still provided beneficial effects in various applications. This point is greatly supported by a study encapsulating gliadin protein with PLGA using a double emulsion with two times of 100% amplitude sonication to produce a NP at a size of 529 ± 6.4 nm [89]. The activity of the protein to reduce inflammatory and enteropathy response was retained in three different celiac disease mice models [89]. Notably, a phase I clinical trial and a double-blinded randomised phase II trial have been completed for this NP (NCT03486990, and NCT03738475, respectively).

However, we still suggest that low to moderate amplitude sonication (e.g., lower than 50% amplitude) with an ice bath in the double emulsion is beneficial for preserving BD activity. Future studies can assess the effect of sonication time on the dispersion of the droplets in emulsion and the enzymatic activity after the sonication. The impact of prolonged sonication over an ice bath on BDs activity and structure is also something to consider.

Table 2. Summary of double emulsion studies for BD encapsulation in the last 5 years.

Encapsulated compounds	Polymer	Surfactant or second polymer(s)	Applications	Size	Encapsulation efficiency, %	Loading capacity, %	Sonication settings	References
Lysozyme	mPEG	/	Infection	~ 180–220 nm	2.4	4.78	15 s followed by 30 s on ice, amplitude not included	78
siRNA, paclitaxel and G0–C14	PEG-PLA	PVA as a stabiliser	Anti-cancer	140.5 ± 1.67 nm	91.03 ± 4.21	/	80 w, 30s followed by 100 w, 2 min	84
Insulin/PEG_{6000}	PLGA	/	Diabetes	240 nm	50	/	50% amplitude, 50%, 1 min	79
8-mer Smac peptide and a 14-mer cell penetrating peptide	PLGA-$mPEG_{2000}$	/	Anti-cancer	197~140 nm	48	2.4	30% amplitude for 30 s followed by 10% amplitude for 1 minute, 3 min	80

KPV/PLGA	Chitosan-coated with HA	PVA as a stabiliser	Ulcerative colitis	272.33 nm	39.7 ± 3.6	/	6 x 10 s, amplitude not included, 30 s followed by 10% amplitude 1 minute	81
Oxidation-resistant griffithsin	PLGA	PVA as a stabiliser	HIV-1 infection	98.5 ± 37.2	48.9 ± 12.7	48.9 ± 12.7 ug/mg	Did not specify	83
siRNA	PLGA-FA-PEG	/	Liver cancer	~90 nm	64.3± 5.6	/	80w for 2 min x 2 times, and 10 s x 6 times	85
Catalase	PLGA-PEG	PVA or CHA as stabilisers	Neurotherapeutic	For CHA: 58.4–70.8 nm For PVA: 109.8–113.3 nm	/	/	Sonicated for 15, 30, and 60 seconds for different groups, amplitude not included	88

cdGMP	PLGA	1, 2-Distearoyl-sn-glycero-3-phosphoethanolamine -PEG-Maleimide	Middle East Respiratory Syndrome Coronavirus	114.0 nm	~48%	/	40% amplitude for 1 min, followed by 30% amplitude for 2 mins	[86]
Vancomycin	PLA-PLGA	PVA as a stabiliser	Antibacterial	312 nm	53 ± 7	25 ± 3	40% amplitude for 15 s for the first emulsion, 40% amplitude for 30 s	[87]
Gliadin protein	PLGA	poly(ethyl methacrylate) or PVA	Anti-Celiac Disease	529 ± 6.4 nm	/	10.8 ± 1.5	100% amplitude for 30 s x 2 times	[89]

2.2.2. Use of emulsifier/stabiliser in double emulsion

In food science, stabilisers or emulsifiers alongside sonication during the emulsion process favour protein stability [90]. However, for drug delivery, the stability of BD is questionable during different emulsion processes. How the stabiliser combined with sonication will affect, BD remains unknown [91]. Some emulsion processes include more than two types of emulsifier and stabiliser. In addition, sonication produces transient bubbles that may induce reactive free radicals production, leading to minor side chain changes of the BD [92]. Although there is still no systematic evidence showing that such altered protein structures affect their function, whether the composition of the stabiliser and the organic phase in the presence of free radicals affect BD activity also deserves further investigation [90].

Admittedly, emulsion is one of the most established and widely used synthesis methods, with over 50 % EE in most cases. However, parameters such as the extended exposure period of the BDs to the solvent in the emulsion also make it debatable whether the BDs can still perform their function. The current review suggests that a low temperature, amplitude and time of less than one minute can still keep the BDs functioning. But further exploration of the BDs secondary and tertiary structure after using sonication and emulsifier/stabiliser is needed to support this suggestion. Moreover, we suggest that excessive exposure to the organic phase without rapid emulsion homogenisation during droplet formation may contribute more to BD denaturation than the effect of energetic sonication waves on BD denaturation.

3. Nanoprecipitation

Nanoprecipitation is one of the first drug encapsulation methods developed by Fessi et al. [93] in 1989. At first, it was applied to synthesise polymeric encapsulated particles within 100 to 300 nm. The physicochemical principles of non-protein NPs synthesis using nanoprecipitation, such as the mixing steps and the solvents, have been thoughtfully investigated [94]. Moreover, the path to industrialisation has also been explored, such as modifications on an industrial scale and the establishment of controlled microfluidic systems [95-97]. Therefore, this method is considered to have a high expectation for BD encapsulation due to its simplicity of operation and its ability to avoid exposure to different emulsifiers and surfactants under sonication conditions. **Table 3** summarizes nanoprecipitation studies for BD encapsulation in the last 5 years.

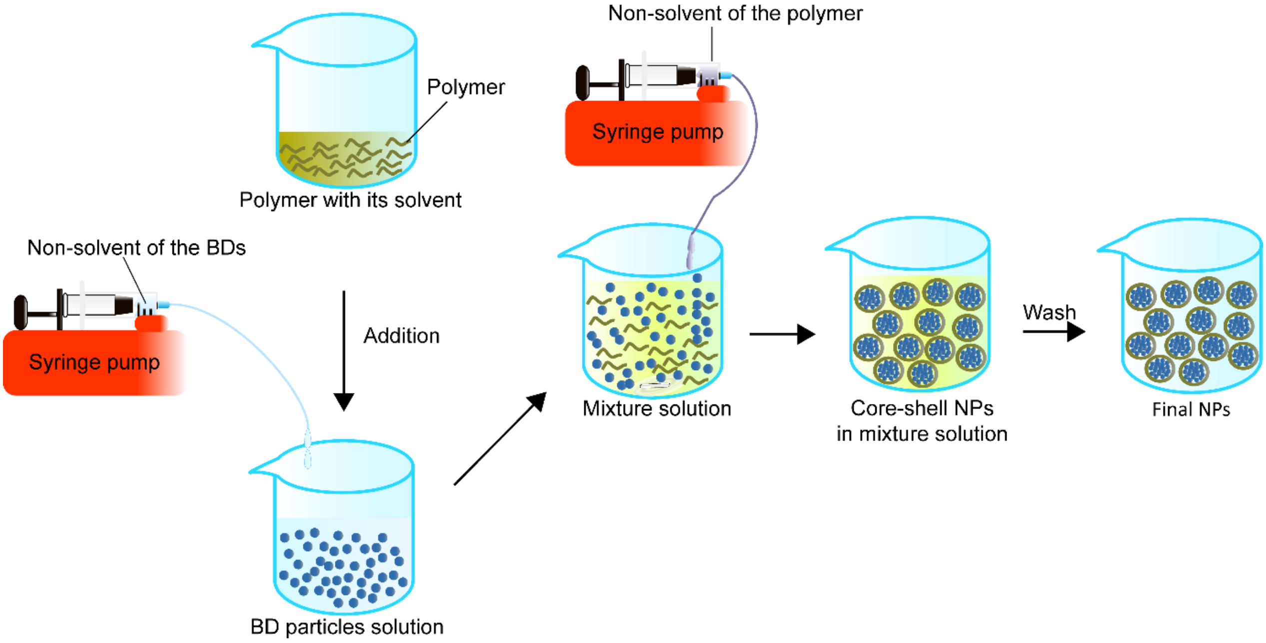

Figure 5. Schematic representation of simple nanoprecipitation to synthesise core-shell nanoparticles.

3.1. Simple nanoprecipitation

A homogeneous core-shell nanoparticle is usually made by dropwise addition of the non-solvent solution of BD to the dissolved BD solution first, followed by the addition of the polymer in its solvent to the BD particle solution. While the mixture of the BD particles and polymer solution is stable, the non-solvent of the polymer can be added to the mixture solution under appropriate conditions such as stirring to form the BD-polymer core-shell NPs (**Figure 5**).

In 2012, Morales-Cruz et al. [98] employed a two-step precipitation method to encapsulate lysozyme and α-Chymotrypsin. They demonstrated that acetonitrile could prevent irreversible denaturation of proteins during the first precipitation process, which might happen when using DMSO. Also, PLGA is soluble in acetonitrile, so the mixture of both protein precipitated particles and PLGA are miscible with each other. Later, when the mixture was added to water, PLGA automatically precipitated and wrapped around the precipitated proteins to form core-shell NPs. Their results indicated that this method had a theoretical protein LC of about 2% or 5% and achieved an EE of 94 ± 5% for lysozyme and 74 ± 4% for α-Chymotrypsin. The size of the lysozyme-loaded PLGA NPs was 336 ± 40 nm, and the α-chymotrypsin-loaded PLGA NPs were 440 ± 16 nm. Two-step precipitation did not impact the residual activity of lysosomes but influenced α-Chymotrypsin. The residual activity of α-Chymotrypsin decreased to 49%, while lysosome activity was 100%. They then encapsulated a horse heart cytochrome c (Cyt-c) with PLGA. After encapsulation, the residual activity was 2% higher than precipitation

(96%). The particle size was 242 nm with 72 ± 2% EE. Although they showed α-Chymotrypsin NPs were cytotoxic to human cervical cancer cell lines, there was no comparison of the effect of NPs with the free α-Chymotrypsin and existing anticancer agent.

Nelemans et al. [99] recently optimised a drug delivery system to encapsulate BSA and amylase with PLGA. This study first showed that only acetonitrile could precipitate BSA with a homogeneous particle distribution while acetone and ethanol caused heterogeneous particle distribution. They found the particle size of BSA varied linearly when increased it from 10 mg/ml to 25 mg/ml with 5 mg/ml increment (35.2 ± 0.2 ± 0.2 nm, 46.2 ± 7.4, 54.3 ± 1.5 and 67.0 ± 4.1 mg/ml respectively). Only 2 mg/ml amylase was used for precipitating a 133.7 ± 4.2 nm particle. The authors eventually encapsulated amylase with PLGA and 1% Pluronic F68 (Diameter: 147.7 ± 4.3 nm, including a 14 nm PLGA shell). However, Nelemans et al. [99] only encapsulated about 24 ± 11.2 % of the amylase into the PLGA NPs. They tested the initially precipitated proteins for activity by directly dissolving the proteins in PBS. The activity of the redispersed amylase was 1.1% higher than its stock solution. This result supported the view that using organic solvents such as acetonitrile to precipitate BDs does not hinder its efficacy.

Queiroz et al. [100] reported a different type of nanoprecipitation. Using a whey protein conjugated chitosan as a shell, they loaded trypsin inhibitor isolated from tamarindo seeds (TTI). Instead of forming TTI particles first to keep it stable, they combined the TTI with the shell complex. Then Tween 80 contained ethanol solution was proportionally added to the solution. A core-shell structure of 109.40 ± 7.53 nm in diameter was formed by homogenising at 17500 rpm with an EE of 98.5 ± 1.95%, and no LC was reported. This work demonstrated that the use of stabiliser and homogeniser in simple nanoprecipitation might not impact the performance of NPs. Also, the TTI encapsulated NPs showed higher *in vitro* antitrypsin activity than the free TTIs at 40°C and 60°C. When the pH was increased from 2.0 to 6.0, the TTI encapsulated NPs still had better antitrypsin activity than free TTI. However, their fourier transform infrared spectroscopy results showed several more vibrational bands than free TTI, suggesting that an underlying chemical reaction has occurred. Overall, such an interaction may not be sufficient to change the activity profile of TTI, but it is worth exploring whether the secondary and tertiary structure of TTI after encapsulated within the NP.

Furthermore, it is worth considering the effect of nanoprecipitation on BD activity compared to other methods. For example, Liao et al. [88] synthesised catalase-loaded PLGA-PEG NPs using the double emulsion method with sonication and nanoprecipitation method. Although there was no significant difference in particle size when comparing NPs prepared by nanoprecipitation and double emulsion method with sonication, there was a significant reduction in catalase activity between the group using nanoprecipitation and the group using emulsion with 30 seconds sonication. Especially for the PVA as surfactant groups, nanoprecipitation-prepared NPs were 35 units/ml lower in catalase activity than the NPs synthesised from double emulsion with 30 seconds of sonication [88]. Notably, the precipitation method that Liao et al. [88] used to compare was a one-step nanoprecipitation that did not precipitate catalase in NP form before mixing the catalase with the PLGA-PEG/acetone solution. Combined with the conclusion from Nelemans et al. [99], the acetone solution in PLGA may impact both distribution and activity of catalase.

Taken together, the selection of non-solvent of BDs and polymers during the nanoprecipitation process contributes to the activity and characteristics of its final product. To gain a more comprehensive understanding of BDs precipitation, small-sized BDs such as siRNA can be used for future studies. Following that, the secondary and tertiary structure of the precipitated large, or small-size BDs can be examined to see whether solvent such as acetonitrile causes any changes on their active sites. Future studies could also determine the impact of different organic solvents on BDs structure. In addition to the future suggestions, works reviewed above on simple nanoprecipitation reported fluctuated EE and did not report their LC. However, nanoprecipitation is a much simpler process than double emulsion, allowing appropriate size control of the NPs.

3.2. Flash Nanoprecipitation

Flash nanoprecipitation is used to reduce the effect of non-solvent on BD. While regular flash nanoprecipitation is used to encapsulate hydrophobic cores, recent studies have utilised a similar principle to encapsulate hydrophilic cores, particularly BDs, in a process called inverse flash nanoprecipitation (iFNP) [101-103]. In particular, iFNP first dissolves BD and polymer in solution form, meanwhile adding non-solvents of the polymer and ionic crosslinker to a mixing chamber such as confined impinging jets (CIJ) or multi-inlet vortex mixer (MIVM) to synthesise NPs that are more homogenised than the conventional precipitation within seconds (**Figure 6**) [104, 105]. This method is considered to have a higher loading and EE than emulsification and conventional nanoprecipitation [101].

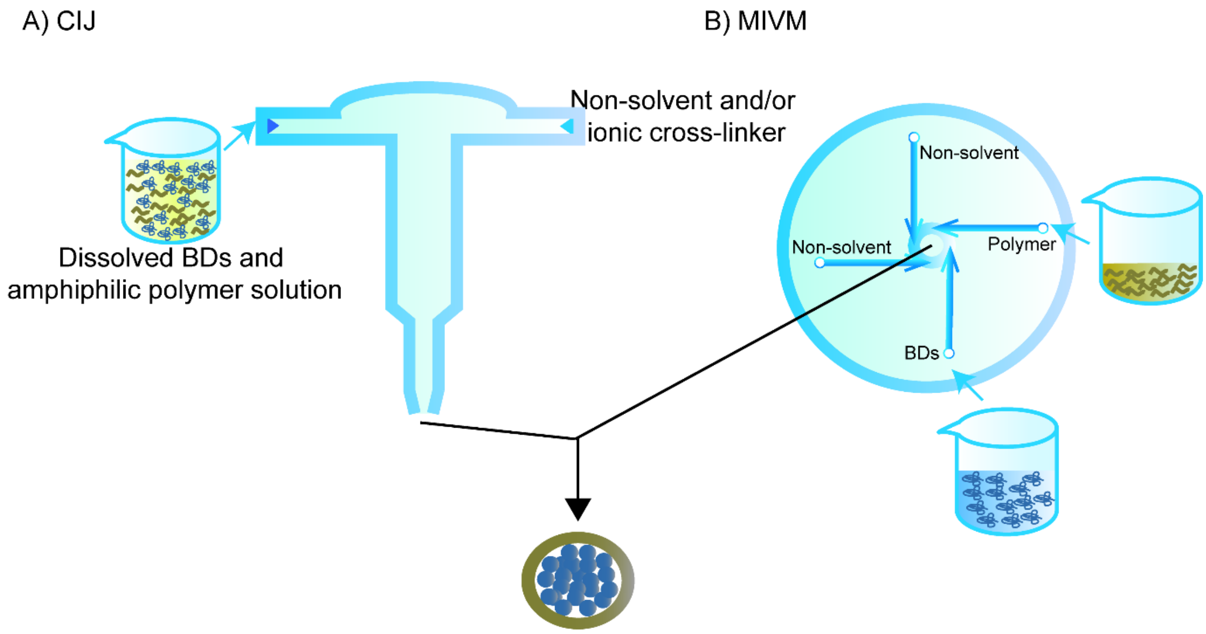

Figure 6. Schematic representation of inverse flash nanoprecipitation(iFNP) to synthesise simple core-shell nanoparticles. (A) The confined impinging jets (CIJ) and **(B)** A multi-inlet vortex mixer (MIVM). The NPs synthesised by iFNP is only a schematic sample, not the actual size.

Since Pagels and Prud'homme [103] introduced the use of iFNP for BD delivery in scaffolds. The group has intensively investigated the possibility of using iFNP to produce BD-polymer core-shell. They encapsulated tobramycin, peptide I, tryptophan, lysozyme, vancomycin, and glutathione separately using a CIJ [103]. DMSO was used as a solvent for both the tobramycin and poly(n-butyl acrylate)-b-poly(acrylic acid), and 5 % H2O was used for better dissolving peptide-I and vancomycin, while 5% H2O and 5% acetic acid was added to the DMSO for tryptophan. The non-solvent chloroform for all of the groups except for tobramycin, acetone was quickly added to the other side of the CIJ. The diameters of the capsulated NPs were all within 200 nm. The group also used transmission electron microscopy to confirm the core-shell structure that was hypothesised for NPs prepared by iFNP containing hydrophilic cores and hydrophobic shell.

In a later study, they also used CIJ to encapsulate vaccine antigen ovalbumin (OVA) with PS-b-PEG and obtained a 147 ± 3 nm NP with 50% LC [102]. They also used MIVM for OVA loading in PS-b-PEG and achieved a size of 115 nm. In addition, a NP using PS-b-PEG to encapsulate horseradish peroxidase (HRP) was synthesised with a size of 167 nm 30% LC. However, the authors did not report the EEs for all prepared NPs. Despite that, this design only required 0.2 mg (200 µl of 1 mg/ml) of the BDs for each encapsulation run, while other studies such as Levit et al. [106] need to use at least 0.9 mg of BSA for preparation. Markwalter followed up with a PLGA - poly(aspartic acid) [PASP] shell to encapsulate polymyxin B, HRP, lysosome, blue

Dextran, vancomycin, RNA and β-galactosidase [107]. PASP has been employed in numerous biomedical applications such as drug delivery[108]. For both CIJ and MIVM settings, they timely added solvent and anti-solvent with ion-crosslinker solution to different mixer entries. Later the primary BD/PLGA-PASP core-shell NPs in its non-solvent were incubated in an aqueous buffer. The aqueous phase was extracted for EE analysis. The primary NPs in its non-solvent were heat-treated to evaporate the previous solvent, then a second copolymer, PLA-b-PEG in tetrahydrofuran, acetone or acetonitrile, was added to be the new solvent. The solution contained the primary NPs, and the second polymer was injected into a new mixer, and an aqueous non-solvent stream was added to the other inputs for a second iFNP. The PLA in the second polymer was self-assembled on the surface of the primary NPs, and the PEG tail provided a strong stability effect. They also simplified the process by directly using a PASP-b-PLA-b-PEG triblock polymer, and BDs dissolved in DMSO then acetone as the non-solvent with an ion-crosslinker. When using a higher molecular weight PLA block, the NPs had sizes of 119 ± 7 nm, 76 ± 2, 114 ± 14 nm, 167 ± 18 nm, 107 ± 16 nm, 70 ± 6 nm, 130 ± 26 nm for encapsulating polymyxin B, HRP, lysosome, blue Dextran, vancomycin, RNA and β-galactosidase, respectively. EE and theoretical LC values were presented in Table 3. This study offered the idea of a hydrogel as a core polymer followed by crosslink hardening of the intermediate polymer to sequester BDs in the polymer shell better. The study highlighted the importance of using a crosslinker during BDs encapsulation. The absence of crosslinker can sometimes result in a loose shell, which may increase the likelihood of package escape. For example, they have shown that polymyxin B without the NH3 as a crosslinker was 40 nm larger than that with the crosslinker. Without the crosslinker, they did not provide EE and LC results for polymyxin B. Nevertheless, we expect the result to be lower than those with the crosslinker. Zeng et al. [109] also employed MIVM to load insulin with a natural linear polymer, HA, for oral delivery. Ionic surfactant dimethyl-dioctadecyl ammonium bromide (DDAB) was used to provide a hydrophobic ion pair with insulin for better encapsulation. The team designed three nanoparticles for 45 nm [109]. The nanoparticles obtained an EE of 94.2 ± 1.8% and an LC of 13.2 ± 0.6%. The authors also tested the NPs in a diabetes rat model. The NPs provided sustained release of insulin within a 9-hour timeframe, thus offering a better blood glucose concentration reduction than insulin solution and insulin powder capsule in a rat model.

McManus et al. [110] used a CIJ mixer to perform iFNP to load insulin and soybean trypsin inhibitor with over 98% EE for oral delivery. The study used two flash precipitation steps. The first was done using a non-degradable polystyrene-b-polyacrylic acid (PS-b-PAA) to load insulin and soybean trypsin inhibitor. Then, a MIVM was used to form one more layer with hydroxypropyl methylcellulose acetate-succinate (HPMCAS) polymer and sodium caprate. In theory, double encapsulation protects the hydrolysis before reaching the target sites, allowing for passing the protein through the gastric barrier and stably releasing the encapsulated protein to reduce blood sugar and the inhibitor to avoid degradation of the NPs in the mucus barrier. Further *in vitro and in vivo* studies are required to assess the effect of double-layer protection.

Overall, flash nanoprecipitation is better at encapsulating BD, and the EE is higher than simple nanoprecipitation. This is most likely due to the high speed of encapsulation compared to simple nanoprecipitation. Flash nanoprecipitation allows more precise control of the process conditions than emulsification, which could be helpful for future large-scale production and faster translation to clinical use. However, there are similarities between flash nanoprecipitation, simple nanoprecipitation, and the emulsification method where organic solvents are used. The effects of organic solvents on BD have been discussed in the previous section, and future studies should try to carefully examine the effects of organic solvents used on therapeutic outcomes for each BD.

Table 3. Summary of nanoprecipitation studies for BD encapsulation in the last 5 years.

Precipitation types	Encapsulated compounds	Polymer	Second polymer or stabiliser(s)	Applications	Size	Encapsulation efficiency, %	Loading capacity, %	References
Simple nanoprecipitation	Lysozyme and α-chymotrypsin	PLGA	/	Improving protein delivery, specific disease application not specified	Lysozyme-loaded: 336 ± 40 nm α-Chymotrypsin loaded: 440 ± 16 nm	Lysozyme-loaded: 94 ± 5 α-Chymotrypsin loaded: 74 ± 4	Theoretical loading: 5	[98]
Simple nanoprecipitation	Amylase	PLGA	Pluronic F68	Immunotherapeutic	147.7 ± 4.3 nm	24 ± 11.2	/	[99]
Simple nanoprecipitation	Trypsin inhibitor isolated form tamarindo seeds	Whey protein conjugated chitosan	Tween 80	Obesity related inflammatory response	109.40 ± 7.53 nm	98.5 ± 1.95	/	[100]
Simple nanoprecipitation	Catalase	PLGA-PEG	CHA or PVA	Neurotherapeutic	For CHA: 58.4–70.8 nm For PVA: 109.8–113.3 nm	/	/	[88]

Flash nanoprecipitation	Ovalbumin or HRP	PS-b-PEG	-	Improving protein delivery, specific disease not specified	115 nm	/	50	102
Flash nanoprecipitation	Polymyxin B, HRP, lysosome, blue Dextran, vancomycin, RNA and β-galactosidase	PLA-b-PASP or PASP-b-PLA-PEG	PLA-b-PEG as stabilising coating when using PLA-b-PASP for encapsulation	General delivery	Polymyxin B loaded: 119 ± 7 nm HRP loaded: 76 ± 2 Lysosome loaded: 114 ± 14 nm blue Dextran loaded: 167 ± 18 nm vancomycin loaded: 107 ± 16 nm RNA loaded: 70 ± 6 nm β-galactosidase loaded: 130 ± 26 nm	Polymyxin B loaded: 80 ± 2% HRP loaded: 82 ± 4% Lysosome loaded: 98 ± 0.4% blue Dextran loaded: 50 ± 5 vancomycin loaded: 12 ± 4% RNA loaded: 48 ± 7% β-galactosidase loaded: not reported	Polymyxin B loaded: 27% HRP loaded: 18% Lysosome loaded: 19% blue Dextran loaded: 7% vancomycin loaded: 2% RNA loaded: 11% β-galactosidase loaded: not reported	107

Flash nanoprecipitation	Insulin	HA	DDAB	Diabetes	45 nm	94.2 ± 1.8	13.2 ± 0.6	[109]
Flash nanoprecipitation	Insulin and soybean trypsin inhibitor (SBTI)	PS-b-PAA	HPMCAS, Chitosan, PEG,	Diabetes	Coated with HPMCAS: 322 ± 6 nm Coated with Chitosan: 321 ± 17 nm Coated with PS-b-PEG: 172 ± 8 nm iNCs/HPMCAS/Zn/C10: 486 ± 60 nm	>98	/	[110]

4. Self-assembly methods

Self-assembly is the spontaneous generation of ordered core-shell structures through local interactions between a BD core and polymeric shell [111]. The interactions include non-polar linkages such as van der Waals forces, electrostatic forces, hydrogen bonding, π-π aromatic stacking, and hydrophobic forces. Past studies mainly used hydrophobic polymers with hydrophobic chemicals for self-assembly [112]. **Figure 7** shows one of the possible representative approach for synthesising BD-loaded core-shell nanoparticles [113]. **Table 4** summarises self-assembly studies for BD encapsulation in the last 5 years.

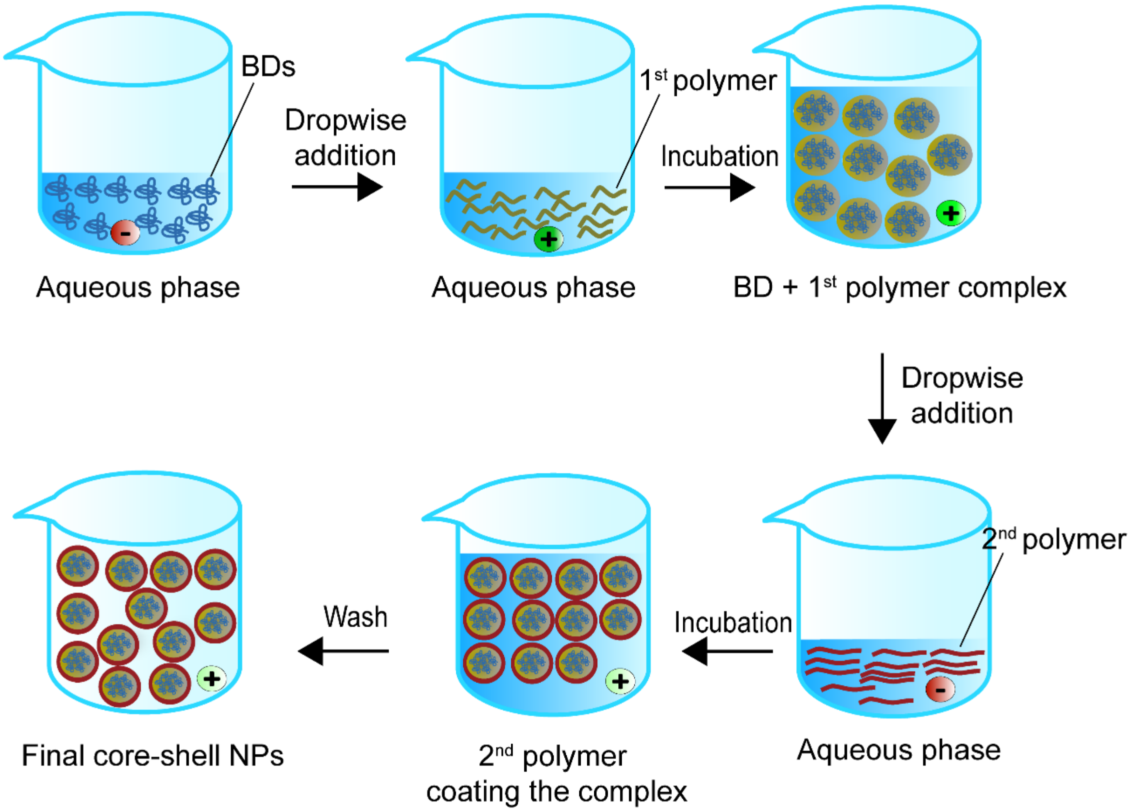

Figure 7. Schematic representation of self-assembly method to synthesise core-shell nanoparticles.

In terms of protein or enzyme encapsulation, Larnaudie et al. [114] designed a drug delivery system with cyclic peptide CP(CPAETC)2 as the core and poly(2-(diisopropylamino)ethyl methacrylate) (pDPA) as the shell to form a 14 nm core-shell sphere at physiological pH. The paper only reported preliminary results and looked at the size and some physical properties of this new material. Later, Lee et al. [115] employed a polysaccharides polymer, dopa-derivatised HA, to synthesise superoxide dismutase (SOD) loaded spherical NPs. Next, inorganic ultra-small size calcium phosphate (USCaP) nanocrystals were produced *in situ* on the spherical NP surface for a more efficient uptake in liver injury treatment. The final particles had an average diameter of 221.1 ± 13.1 nm and 73.4% EE [115]. The authors suggested that the results gave an insight into the future use of different catechol-derivatised hydrophilic polymers(CDHPs) for surface charge management in different biomedical applications. The work reported both *in-vitro* and *in-vivo* experiments. In this study, the cytotoxicity of the NPs was evaluated in vitro only without examining whether the NPs would cause damage to organs in *vivo*. A limitation of these NPs is that SOD encapsulated HA NPs should not be used in people with liver diseases. This is because serum HA is an important clinical non-invasive biomarker of liver fibrosis for chronic liver diseases such as chronic hepatitis infections and cirrhosis [116]. For example, in cirrhosis or hepatitis C patients, the level of HA is higher than in healthy humans because of the patients had increased liver fibrosis [117, 118]. Therefore, increasing the HA level at this time may obscure the true extent of liver damage of the patient and mislead clinical management [118-120].Mei et al. [121] used mixtures of anionic poly(acrylic acid) (PAAc) and tPA in combination with cationic poly(ethylene glycol)-b-poly[4-(2,2,6,6-tetramethylpiperidine-1-oxyl)aminomethylstyrene] (PEG-b-PMNT) di-block amphiphilic copolymers to form nanoparticles in water using hydrophobic polycations. The copolymer had 4-amino-2,2,6,6-tetramethylpiperidine-1-oxyl (4-amino-TEMPO) on its side chains, which controls the reactive oxygen species, to aid the treatment. The team showed that their particles were effective compared to free tPA in reducing brain infarct volume and improving neurobehavioral results in a stroke mouse model. Furthermore, the prepared particles also reduced the area of tPA-induced subarachnoid haemorrhage by about 10% compared to free tPA, thus demonstrating that the particles could improve the brain haemorrhage previously caused by the use of tPA. However, the authors also did not report the LC and EE and whether this method is comparable to other encapsulation methods. Moreover, the representative images and the infarct volume results of the free tPA and tPA NPs without TEMPO group were very similar. The particles with TEMPO showed a lower infarct volume compared to the group with encapsulated tPA without TEMPO. The same happened for the haemorrhage area results between the two treatment groups. Also, the subarachnoid haemorrhage area of the tPA without TEMPO groups was not significantly different to the free tPA treatment. Combined altogether, TEMPO may have a higher therapeutical value than tPA and the redox NP shell.

Despite that, Zhang et al. [122] also used a self-assembly method to load urokinase (UK) within an adamantane (ADA) conjugated fucoidan shell. The core contained tirofiban and a loaded small molecule peptide named LSIPPKA in PLGA beta-cyclodextrin (β-CD) NPs. Then UK was added to the β-CD, and LSIPPKA modified PLGA aqueous solution. The final core-shell NPs with ADA-fucoidan shells were formed via the host-guest inclusion interaction of β-CD and ADA in an aqueous solution (**Figure 8**). The size of the nanoparticles was larger (575.6 nm) compared to other studies due to the double layers. LC and EE were reported as 22.89% and 62.61%, respectively.

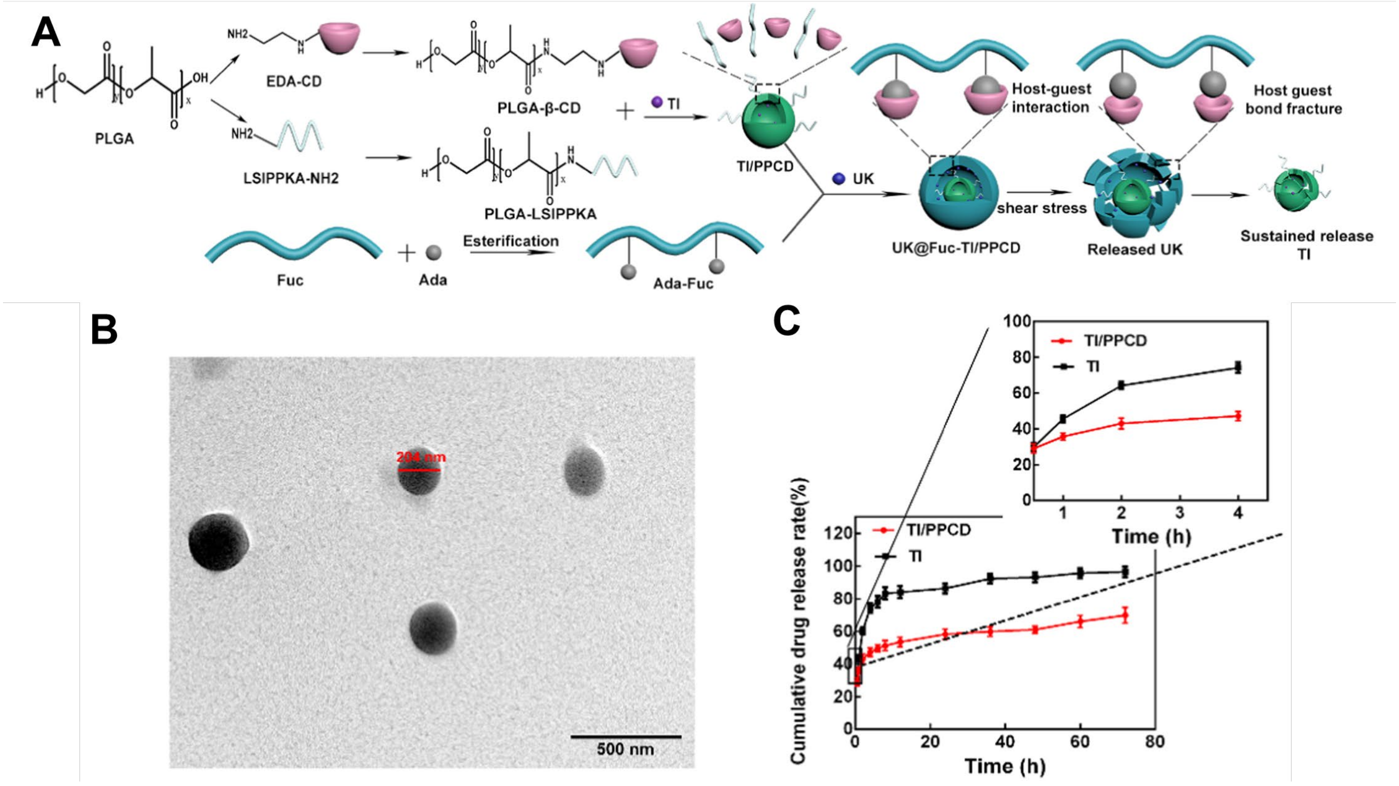

Figure 8. Synthesis route, thrombolytic mechanism and characteristics of UK@Fuc-TI/PPCD. (A) The synthesis route and drug release mechanism of **urokinase** UK@Fuc-TI/PPCD, **(B)** TEM image of UK@Fuc-TI/PPCD NPs after shearing (1000 dyne/cm^2) for 20 min. **(C)** The sustained release profile of TI from TI/PPCD cores in PBS medium and free TI was used as the control. Reprinted from Ref. [122], copyright (2021), with permission from Elsevier.

Ma et al. [123] employed a novel plant-derived p-hydroxyphenylethyl anisate and 3-acrylamidophenylboronic acid to form a shell to load insulin for diabetic treatment. Insulin core was self-assembly encapsulated to the shell. As the NPs had good EE and LC (65% 16%, respectively), it indicates that this novel polymer is promising for BD-encapsulated polymeric transportation. The NPs provided sustained insulin release for up to 28 hours in a diabetic mouse model. They had good biocompatibility that did not cause histological differences in major organs and did not show notable *in vitro* and *in vivo* toxicity after 14 days of injection.

Levit et al. [106] combined iFNP with self-assembly to encapsulate BSA. They first formed a BSA-Tannic acid (TA) bound complex in the presence of an amphiphilic block copolymer stabiliser, polystyrene-b-polyethylene glycol (PS-b-PEG) in a CIJ mixer. They then employed 10 kDa polyethylenimine (PEI) to coat the complex via electrostatic interaction to form a core-shell NP . They claimed that TA did not affect the size or zeta potential but only helped increase LC. In BSA-TA-loaded NPs with 10 kDa PEI, the addition of TA increased the EE from 8 ± 3% to 79 ± 7% and LC from 1% to 13 ± 1%. Interestingly, when using a higher Mw PEI (750 kDa), an aggregate complex formed with a decreased EE by 29% and LC by 5% compared to PEI at 10 kDa. In this work, TA-BSA complex was formed by hydrogen bonding. The authors did not assess whether the binding of TA affected BSA. Moreover, it might be an issue if the model protein BSA is replaced by therapeutic BDs in the future, because hydrogen bonds might be critical for BD's functionality. Namely, hydrogen bonds are actively involved in potential therapeutic targets or receptors of various diseases, such as Severe Acute Respiratory Syndrome Coronavirus-2 (SARSr-CoV2) infection, Alzheimer disease, and cardiovascular diseases [124-128]. So binding TA or other agents with BDs via hydrogen bonds in the future may need a case-by-case analysis. We suggest that self-assembly may reduce the effect of BD structure changes that may happen in emulsion methods. However, the EE in this method may be lower than in those in other methods because the interaction forces between the self-assembled particles are weaker than those of particles synthesised by other methods. A major problem with the self-assembled polymeric drug delivery system is that the ionic interactions affect the NPs stability. The ion strength between the core-shell is heavily impacted by concentration, and a diluted concentration may cause the structure to collapse [129]. Thus, research has worked on applying other aids to overcome the loading problem in self-assembly. In particular, the NP developed by Cheng et al. [130] carried insulin with poly(n-butylcyanoacrylate) for oral delivery. The dispersibility of poly(n-butylcyanoacrylate) was enhanced by the addition of sodium dodecyl sulfate (SDS), whereas poloxamer 407 was used to raise the physical stability of the NPs for crossing intestinal mucus layer. Following the addition of these stabilisers, 3 minutes (2s on and 3 s off) at 200W sonication was used for better loading the insulin. The authors claimed that stabilisers and sonication did not impact insulin activity. The size of the NPs was about 140 nm. The study showed a sustainable insulin release and blood glucose level compared to the free insulin injection group. Future studies can follow up on the LC and EE of these particles to enrich their profiles and thus increase the credibility of using the self-assembly method to synthesise BD-polymer core-shell NPs.

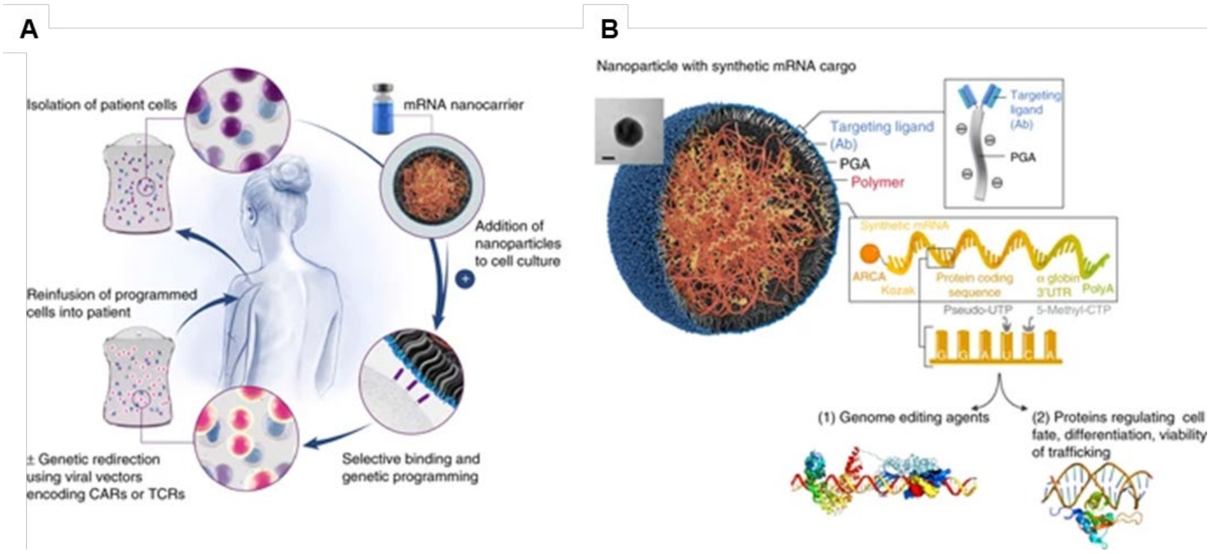

Figure 9. mRNA nanoparticles to program therapeutic T-cells. (A) Scheme explaining how cultured T-cells can be programmed to express therapeutically relevant transgenes carried by polymeric NPs. These particles are coated with ligands that target them to specific cell types, enabling them to introduce their mRNA cargoes and cause the targeted cells to express selected proteins (like transcription factors or genome-editing agents). **(B)** Design of targeted mRNA-carrying NPs. The inset shows a transmission electron micrograph of a representative NP; scale bar, 50 nm. Also depicted is the synthetic mRNA encapsulated in the NP, which is engineered to encode therapeutically relevant proteins. Reprinted from Ref. [131], copyright (2017), with permission from Springer nature.

Up-to-date, the potential of the self-assembly method to encapsulate BDs for gene therapy has been extensively explored for various diseases. For example, Smith et al. [132] loaded a negatively charged plasmid with leukaemia-targeted chimeric antigen receptor genes (194-1BBz) and CD3ζ cytoplasmic signalling domains to an overall positively charged poly(beta-amino ester) [PBAE] polymer with microtubule-associated-nuclear localisation peptides. The primary positively charged complex was covered with a negatively charged polyglutamic acid shell with a targeting ligand to form a NP with 155 ± 40 nm diameter. Their show that the lymphocyte antigen-recognised NPs could be translocated to T cell nuclei to prevent disease progression. This study also supports the ability of the self-assembly method to effectively load genetic information compared to the free gene group.

Their group also showed the potential of these carriers in mRNA delivery via self-assembly [131] (**Figure 9**). Synthetic mRNA was attached to the positively charged PBAE to form a complex, and then the complex was coated with an antibody-functionalised PGA to form an NP at a size of 109.6 ± 26.6 nm. They demonstrated that their self-assembled NPs had better viability, T-cell expression, and knock-out efficiency than the conventional electroporation for transfection. Moreover, the encapsulated mRNA can be encoded with other transcription factors for anti-tumour purposes and programmed for hematopoietic stem cells self-renewal.

Karlsson et al. [133] used self-assembly method in acidic environment to load systemic siRNA in modified PBAE with extra disulfide bonds to enhance intracellular release of the siRNA for brain glioblastoma treatment. The study demonstrated that their self-assembled NPs *(~57 nm)* could cross the barrier via vesicular in an *in vitro* simulated blood-brain barrier model. In addition, after intravenously injecting the NPs, a significantly higher amount of the NPs was found in the brain of cancer-bearing mice compared to control, without affecting the integrity of the blood-brain barrier. Other studies with self-assembly method were also conducted after this one to deliver mRNA to the brain. Yet, they all used intracerebroventricular injection, a method to bypass the blood-brain barrier by injecting the NPs directly into the cerebrospinal fluid (see **Table 4** for details of size and other parameters of the studies) [134-136]. We suspect this injection method was chosen to avoid the early release of self-assembled NPs due to ionisation or acid-base conditions. However, intracerebroventricular injections are prone to infection, bleeding, malposition and increased probability of nosocomial infections due to their catheter placement in clinical contexts, and should therefore be noted for clinical translation [137]. Given that Karlsson et al. [133] have demonstrated that self-assembled NPs at small size can cross the blood-brain barrier via a transcytosis by a vesicular mechanism, future studies could try subcutaneous injection of self-assembled NPs for brain diseases.

A recent paper reported a NP at a size of 300 nm using a cationic core consisting of a hyperbranched cationic polyamide-amine-peptide-amine (HPAA-peptide-Fc) bonded siRNA complex and coated by an anionic hyperbranched polyglycerol ether (HPG)-modified β-cyclodextrin derivative (CD-HPG) shell for cancer therapy [138]. After the core polypeptide complex formed, the siRNA siPLK1 was dissolved and bound to the complex in a complex aqueous solution with the help of ultrasonication. The aqueous shell solution was added to the cationic siPLK1 contained complex for self-assembly NP formation. The particles were effectively down-regulated Plk1 protein expression in breast cancer cells. However, these cancer-focused studies did not report the EE and LC of the methods. This raises a further concern that the method has relatively low loading and also concerns about the stability of the encapsulated BDs. Double-stranded RNA could also be encapsulated via the self-assembly method. The RNA was first mixed with an epigallocatechin gallate to form a complex, then encapsulated by Poly-l-lysine under 30 minutes vortexing and 5 minutes sonication in distilled water[139]. With the aid of the polymer, the release period was extended compared to the free

RNA group.

In terms of DNA delivery, Gu et al. [113] synthesised a retro-inverso d-peptide (RIF7)-modified HA/bioreducible hyperbranched poly(amidoamine) (RHB)/plasmid DNA (pDNA) ternary nanoparticles with a size of 193.1 ± 8.72 nm for cancer treatment. The author claimed that the positively charged RHB coated the negatively charged pDNA via electrostatic interaction at a 5:1 weight ratio to form an RHB/pDNA complex. Due to the overall positively charge of the complex, a negatively charged RIF7-HA was employed to coat the complex to decrease the surface charge of the complex for better circulation and targeting effect. Cui et al. [140] utilised electrostatic interactions to synthesise BD-loaded polymeric core-shell for anti-tumour purposes. The team first mixed a gene called programmed cell death protein 4 (PDCD4) with a cationic poly(cystamine bisacrylamide)-urea-histamine (PCAH) carrier, which was then combined with the anionic polymer dextran-G-anhydride (PDA) to form a particle with a diameter of approximately 110 nm. Compared to the free PDCD4 group, which had a minimum effect similar to PBS, the encapsulated PDCD4 group could reduce 4T1 tumour cell proliferation *in vitro* (100% vs 60%). Consistently, the PDCD4 loaded PCAH NP group had a lower tumour volume than free gene group. These results indicated the importance of the use of a carrier for anti-tumour gene therapy. While this work showed that the NPs effectively increased the transfection efficiency by 5 times as compared to the group without DNA (Mean fluorescence intensity: $3x10^4$) at pH 7, they did not include the transfection results of the free gene group as part of comparison.

Results from studies mentioned above support the idea that self-assembly can encapsulate different genetic material and allow better targeting through polymeric NP carriers. Crosslinkers had been used to stabilise the nanoparticles. PEGylated-chitosan NP (110 nm) was crosslinked by tripolyphosphate to deliver mRNA (miR-206 or miR-223, 60% EE) [141]. The expression of ATP-binding cassette transporters A1 gene in macrophage was reduced both in vitro and in vivo. As a result, the cholesterol transport to plasma liver and feces in this crosslinked NP-treated mice were decreased. Furthermore, we suggest that self-assembly may reduce the effect of BD structure changes that may happen in emulsion methods. However, the EE in this method may be lower than in those in other methods because the interaction forces between the self-assembled particles are weaker than those of particles synthesised by other methods. A major problem with the self-assembled polymeric drug delivery system is that the ionic interactions affect the NPs stability. The ion strength between the core-shell is heavily impacted by concentration, and a diluted concentration may cause the structure to collapse [129]. Thus, research has worked on applying other aids to overcome the loading problem in self-assembly. In particular, the NP developed by Cheng et al. [130] carried insulin with poly(n-butylcyanoacrylate) for oral delivery. The dispersibility of poly(n-butylcyanoacrylate) was enhanced by the addition of sodium dodecyl sulfate (SDS), whereas poloxamer 407 was used to raise the physical stability of the NPs for crossing intestinal mucus layer. Following the addition of these stabilisers, 3 minutes (2 s on and 3 s off) at 200W sonication was used for better loading the insulin. The authors claimed that stabilisers and sonication did not impact insulin activity. The size of the NPs was about 140 nm. The study showed a sustainable insulin release and blood glucose level compared to the free insulin injection group. Future studies can follow up on the LC and EE of these particles to enrich their profiles and thus increase the credibility of using the self-assembly method to synthesise BD-polymer core-shell NPs.

Table 4. Summary of self-assembly studies for BD encapsulation in the last 5 years.

Encapsulated compounds	**Polymer**	**Second polymer or stabiliser(s)**	**Applications**	**Size**	**Enc effic**
Cyclic peptide CP(CPAETC)2	pDPA	/	General BD delivery	14 nm	/
Superoxide dismutase	Dopa-conjugated HA	/	Treating drug-induced hepatotoxicity and liver injury	221.1 ± 13.1 nm	73.4
Plasmid DNA	HA	/	Anticancer	193.1 ± 8.72 nm	/
PDCD4	PCAH	PDA	Gene therapy	110 nm	/
Enzyme-responsive polypeptide modified polyamide-amine (HPAA-peptide-Fc)	CD-HPG	HPAA	Anti-cancer	~300 nm	/
tPA	PAAc	PEG and PMNT	Thrombolysis	48 ± 2 nm	/
Urokinase	PLGA	LSIPPKA peptide, beta-cyclodextrin and fucoidan	Thrombolysis	575.6 nm	62.6
Insulin	p-hydroxyphenylethyl anisate	3-acrylamidophenylboronic acid	Diabetes	165.37 nm	~65
Insulin	Poly (n-butylcyanoacrylate)	SDS and poloxamer 407	Diabetes	~140 nm	100
BSA	TA	PS-b-PEG and PEI	Improving protein delivery, not specified	10 kDa PEI: 153 ± 7 nm	10 k ± 7

microtubule-associated sequences (MTAS) and nuclear localization signals and plasmid DNA	PBAE-447	PGA	General gene therapy	155 ± 40 nm	/
Synthetic mRNA	PBAE-	PGA	General gene therapy	109.6 ± 26.6 nm	/
Systemic siRNA	Modified PBAE	/	Brain Glioblastoma	67 nm	/
Luciferase mRNA	PASP	PEG	General intracerebroventicular delivery	34 nm	/
in vitro transcribed mRNA and cotransfected single guide	PASP	/	Cerebral genome engineering	100-130 nm	/
CRISPR-associated protein 9 mRNA and guide RNA	PASP	/	Cerebral genome engineering	64.9 ± 5.1 nm	/
Double stranded RNA	Poly-l-lysine	/	Gene silencing	46.2 ± 8.1 nm	/
SiRNA	Trimethyl and thiolated chitosan	HA	Anti-cancer	110 nm	/
mRNA	Chitosan	PEG	Atherosclerotic lesions	~110 nm	60 %

Coaxial electrospraying

Coaxial electrospray is a novel method to encapsulate BD improving stability and producing small NPs Electrospraying technique is already applied in other areas, such as solar cells with large-scale production settings [144, 145].

A coaxial electrospray includes a coaxial nozzle, a positive electrode applied at the tip of the nozzle, and a negative or ground electrode is connected to the collector to create an electric field. The syringe pump pushes the core and shell material depending on the requirements. The potential difference pushes the liquids out to produce nanoscale particles (**Figure 10**). This technique shares a similar electrohydrodynamic process as electrospinning [146]. Electrospinning produces different morphologies of nanomaterial, such as nanofiber and nano-scaffold to encapsulate chemical drugs and BDs [147-151]. Due to the morphological interests, this review only focuses on the electrospraying method for synthesising BD-loaded polymeric NPs. **Table 5** summarizes coaxial electrospraying studies for BD encapsulation in the last 5 years.

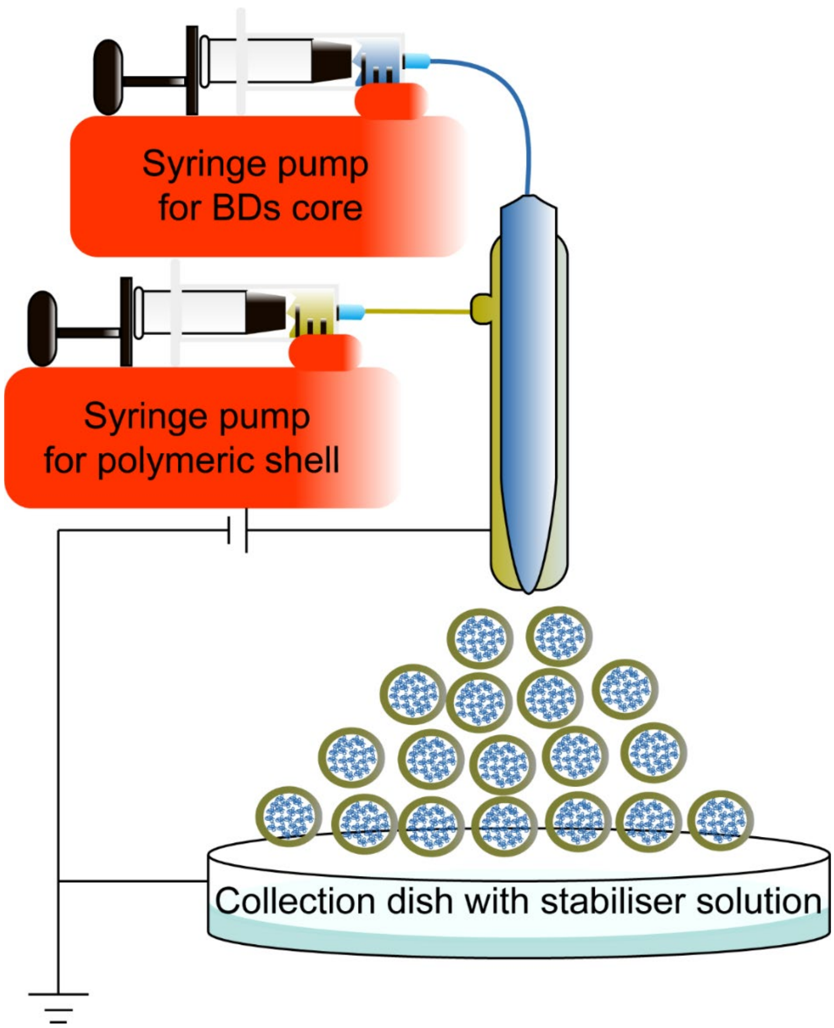

Figure 10. Schematic representation of coaxial electrospraying method to synthesise

core-shell nanoparticles. The NPs synthesised by coaxial electrospray in the scheme are only a schematic sample, not the actual size.

Previous studies have focused on micron-sized BD core-shell encapsulation particles. However, only a limited number of nanoscale BD core-shell encapsulation studies were reported [152]. Yaghobi et al. [153] reported the preparation of streptokinase (SK) loaded PLGA nanoparticles with a size of 37 ± 12 nm, 90% EE, and 8.2% LC. This is a pioneering study of BD-polymer core-shell nanoencapsulation. Subsequently, the team used mPEG-PLGA to encapsulate SK and obtained particles with a size of 194.3 ± 15.9 nm, EE of 83.3 ± 3.2% and LC of 8.2 ± 0.7% [154]. This study demonstrated that NPs prepared by coaxial electrospray did not impact the bioactivity of BD and blood parameters such as red blood cells as well as coagulation factors, compared to free SK. The human umbilical vein endothelial cells and female rats treated with NPs group also had a better result *in vitro* and *in vivo* viability than these in commercial SK. However, the authors did not examine thrombolysis rates, which would provide better evaluation on whether the synthetic nanoparticles were more effective than the free SK. Overall, the BD used in these two articles could be heavily loaded into hydrophobic polymers and form a dense shell. However the synthesised NPs might not be homogenous as reported by Hasanpour et al. [154], this coaxial electrospraying method yielded a polydispersity Index of 0.73 ± 0.015. Future optimisation may be required to obtain more homogeneous nanoparticles.

Furthermore, there has been a disagreement on whether coaxial electrospraying can be used for high throughput production in the industry [155]. This method involves the intervention of electromagnetic fields and potential differences. For example, without good isolation of the magnetic field, some nanoparticles with positive charges interact with the surrounding air but do not drop to the collection plate, reducing the efficiency of coaxial electrospray to produce BD-loaded NPs [156]. It was suggested that using ring electrodes for less distributed cone-jet sprayed NPs is one of the possible solutions [157]. Further studies can also explore establishing a large-scale electronic static isolation shield to favour the mass production of the core-shell NPs.

Table 5. Summary of coaxial electrospraying studies for BD encapsulation in the last 5 years.

Encapsulated compounds	Polymer	Second polymer	Applications	Size	Encapsulation efficiency, %	Loading capacity, %	References
SK	PLGA	/	Thrombolysis	37 ± 12 nm	90	8.2	[153]
SK	PLGA	mPEG	Thrombolysis	194.3 ± 15.9 nm	83.3 ± 3.2	8.2 ± 0.7	[154]

5. Insights for future directions, perspectives, and translation of biomedical applications

Manufacturing methods for BD encapsulation summarised in the previous sections have successfully loaded various BDs such as protein, enzyme, peptide, DNA, mRNA and siRNA. Typical methods to produce core-shell BD-loaded polymeric NPs include single emulsion, double emulsion, simple nanoprecipitation, iFNP, self-assembly and coaxial electrospray. Using polymers to encapsulate BD with a single emulsion method exhibits a low EE and is challenging to control scale-up production. The double emulsion improves the low EE issue of the single emulsion method and has been extensively investigated for various BDs. However, the effects of sonication and organic solvents on BDs have not been fully explored. The simple nanoprecipitation method shows fluctuations in EE for different BDs, and this method also involves organic solvents. iFNP produces core-shell NPs by rapidly introducing a non-solvent of the polymer into the cavity and mixing rapidly. The shortcomings of normal nanoprecipitation, such as the contact time of non-solvent to the BDs and polymer are improved by using iFNP. The self-assembly method also allows for the rapid formation of core-shell structures but can be affected by the concentration dilution, leading to the breakage of the nanomaterial, thus compromising its effectiveness. Coaxial electrospray allows precise control of the variables to achieve high LC and EE. However, coaxial electrospray is susceptible to the influence of surrounding static electromagnetic fields, leading to sample waste and poorly distributed sample results (As summarised in **Table 6**). Therefore, further optimisation should be carried out to address the shortcomings of these methods.

Table 6. Summary of the pros and cons of each synthesis method

Synthesis methods	EE	LC	Advantages and disadvantages
Single emulsion	Low	Low	✓ Commonly used methods that allow uniform shape and size distribution × Use of sonication, stabiliser and organic solvents may impact BDs stability
Double emulsion	Moderate	Low	
Simple nanoprecipitation	EE and LC are impacted by the size of the BDs		✓ Fast and simple to prepare × Use of organic solvents
iFNP			✓ Reduce the contact/reaction time between the BDs and non-solvent improves NPs characteristics × Unknown mixing mechanism
Self-assembly	High	Low	✓ Variety of shape × Package leakage, and pre-release of BDs due to surrounding micro-environment change
Coaxial electro-spraying	High	Low	✓ High encapsulation efficiency × Waste of sample due to collection condition

The combination of microfluidic devices and conventional synthesis methods is a practical approach in advancing BD-loaded polymeric NPs synthesis. Previously, microfluidics has mostly been studied at the micron level for BD encapsulation [158, 159]. However, the summarised iFNP method section supports the use of microfluidic devices in BD encapsulation. However, the summarised iFNP method section supports the use of microfluidic devices in BD nano-encapsulation. Also, there are studies using microfluidic devices with self-assembly mechanism to encapsulate siRNA in 7C1 and PEG2000 polymers NPs and successfully conduct endothelial gene silencing in mice organs [160]. These examples demonstrate the use of microfluidic devices in polymer-coated BDs encapsulation [161]. Further refinement of the devices maybe achieved via modifying the structure of the device to reduce BDs and non-solvent contact and also enhance the mixing ability. For example, the use of Tesla structure in microfluidic device has been shown to benefit insulin encapsulation in PLGA NPs; primary parameters such as flow rate and the concentration of PLGA and insulin does not interfere with the physical characteristics of the produced NPs [162]. Whether these could be translated to general BD-loaded polymeric NPs production with microfluidic devices still needs investigation. Overall, it is suggested that the combination of conventional synthesis methods with microfluidic device, can facilitate the use of polymers for BD encapsulation in the future. The use of microfluidics device is also a potential solution for large-scale production and better control of the conditions under which the nanoparticles are formed. If future studies can overcome the disadvantage of slow production yield, microfluidic-based method will benefit future mass production applications [163].

Furthermore, one of the key challenges that BD faces in drug delivery are releasing, denaturing and clearing before reaching the target site [164, 165]. Future studies can explore other biodegradable materials to refine their properties and compare their effects with the currently available FDA-approved polymers for a more comprehensive understanding. Specifically, FDA-approved polymers, such as PLGA, may not be a suitable polymer shell for encapsulating BD in acute disease treatment [166, 167]. PLGA has a slow hydrolysis profile in physiological pH and temperature that release encapsulated molecules after days to months [166-169], yet some studies targeting acute disease treatment are still using PLGA as a carrier.
It is important to explore other novel polymers that can be used for acute and chronic diseases with minimum modification.

The polymer shell should be modified to tune the hydrolysis rate and drug release profile corresponding to a specific disease. For example, polymeric shell used in cancer or diabetes should have slow dissolution or hydrolysis rate to provide long-term sustained release of the therapeutic compounds. However, in acute diseases such as thrombosis and stroke, the shell should be hydrolysed or degraded quicker to offer sustained release over a shorter period [170].

New type of polymers such as molecularly imprinted polymers (MIPs) can be employed for targeted drug delivery. MIPs are synthetic materials that contain recognition sites for specific binding to potential binding sites in the body [171]. Based on the required disease's physiological condition, functional and crosslinking monomers are selected based on their ability to bind to a template molecule via weak non-covalent or reversible covalent bonds. Cleavage of the bonds between the monomers and template can produce the required MIPS. MIPs can be degraded in physiological conditions with different degradation profiles that allow controlled release with the help of temperature and pH. Also, due to the specificity of the functional monomer, it has a high affinity to the targets [171, 172]. Several studies have demonstrated the potential use of MIPs for the delivery of chemical drugs or other therapeutic agents in biomedical applications. [173-175] It is worth to apply different modifications or inventions to the MIPs for different needs. Using MIPs as novel shells to encapsulate BDs or directly stitching BDs as part of the MIPs into a more stereospecific polymer cocktail will broaden the utility of synthesis methods and the application types [176].

As can be seen from the articles reviewed in this paper, the size of the BDs may impact the efficiency of the encapsulation. For example, in Markwalter et al. [87, 107], vancomycin is typically only 1.45 kDa in size, thus can easily escape from the packaging envelope during the encapsulation process [177]. So far, there are only a few studies encapsulating small molecular weight BDs with polymeric materials. Future explorations can adapt different production methods and materials, such as introducing MIPs for small molecular weight BDs encapsulation to achieve better results for drug delivery. This review believes that the advance of polymeric materials can benefit the established synthesis methods for nanoparticle synthesis.

Janus structure can be considered for polymeric nanoencapsulation for BDs. Janus-structured NPs are particles that contain multiple domains to simultaneously load a combination of drugs for various purposes, such as theranostics and delayed drug release [178-180]. Combining the Janus structure with existing production methods is something that studies have already done. Synergistic analgesia by oral administration of janus-structured NPs using a double emulsion of najanajaatra venom protein and resveratrol has been reported [181]. Also, a study used cellulose acetate and polycaprolactone as carriers to transport sliver NPs and lavender oil [182]. Currently, limited number of studies are using a polymeric carrier to load BDs in a Janus structure. Whether such a structure can be combined with existing production methods and the use of microfluidic devices to benefit BD-loaded polymeric NPs delivery is worth to be explored in the future.

The BD-encapsulated NPs undergoing clinical trials are mainly lipid NPs such as SARSr-CoV2 vaccines, mRNA-1273, BNT162b2, and NVX-CoV2373 that were tested in phase III clinical trials [183-186]. There are limited number of polymeric BD-encapsulated NPs prepared by emulsion methods undergoing clinical trials as discussed in previous sections. Advanced microfluidic devices appear as a new potential and efficient approach to encapsulate BDs within polymeric nanoparticles.

6. Conclusion

This review first discussed the advantages and disadvantages of various available nanomaterials and then discussed the use of polymeric materials for BD encapsulation. Free BD is not efficiently absorbed in the body and is prone to degradation, clearance or aggregation, possibly leading to other complications. Using polymers to encapsulate BD, rather than conjugate BD, allows for better drug delivery by maximising the bioactivity of BD while increasing efficacy. A core-shell structure is preferred to encapsulate BDs due to BD characteristics, high LC, EE, controlled release manner and higher stability of core-shell encapsulation. This review describes the various methods used to encapsulate BD with polymers in recent years.

The information collected in this review is expected to benefit the development of future polymeric NPs for BD delivery by facilitating the selection of synthesis method and suitable polymeric materials. A combination of appropriate improvements to existing methods and development of novel materials could drive the advancement of drug delivery.

7. Abbreviations

BD	Biological drug
BVZ	Bevacizumab
CHA	Cholic/deoxycholic acid
CIJ	Confined impinging jets
CMC	Carboxymethyl chitosan
CP(CPAETC)2	Cyclic peptide
Cyt-c	Cytochrome c
DDAB	Dimethyl-dioctadecyl ammonium bromide
DMSO	Dimethyl sulfoxide
DNA	Deoxyribonucleic acid
EE	Encapsulation efficiency
FA	Folic acid
FDA	Food and Drug Administration
HA	Hyaluronic acid
HA	Hyaluronic acid

HIV-1	Human immunodeficiency virus-1
HPG	Polyglycerol ether
HPMCAS	Hydroxypropyl methylcellulose acetate-succinate
HRP	Horseradish peroxidase
IC50	Half-maximal inhibitory concentration
KPV	Lysine-proline-valine
LC	Loading capacity
M. luteus	*Micrococcus luteus*
MIPs	Molecularly imprinted polymers
MIVM	Multi-inlet vortex mixer
mPEG	Methoxy polyethylene glycol
mRNA	Messenger RNA
NP	Nanoparticles
NY-ESO-1	New York esophageal squamous cell carcinoma 1
OVA	Ovalbumin
PAAc	Poly(acrylic acid)
PAE	Poly (β-amino ester)
PASP	Poly(aspartic acid)
PBAE	poly(beta-amino ester)
PCAH	Poly(cystamine bisacrylamide)-urea-histamine carrier
PDA	Polymer dextran-G-anhydride
HPAA	Hyperbranched cationic polyamide-amine
pDNA	plasmid DNA
pDPA	Poly(2-(diisopropylamino)ethyl methacrylate)
PEG	Polyethylene glycol
PEI	Polyethylenimine
PLA	Polylactic acid
PLGA	Poly lactic-co-glycolic acid
PMNT	Poly[4-(2,2,6,6-tetramethylpiperidine-1-oxyl)aminomethylstyrene]
PS-b-PAA	Polystyrene-b-polyacrylic acid
PS-b-PEG	Polystyrene-b-polyethylene glycol
PVA	Poly(vinyl alcohol)

RHB	Bioreducible hyperbranched poly(amido amine)
RIF7	Retro-inverso d-peptide
RNA	Ribonucleic acid
SARSr-CoV2	Severe Acute Respiratory Syndrome Coronavirus-2
SiRNA	Small interfering ribonucleic acid
SK	Streptokinase
Smac	Second mitochondria-derived activator of caspase
SOD	Superoxide dismutase
TA	Tannic acid
TEMPO	Tetramethylpiperidine-1-oxyl
TK	Thioketal
UC	Ulcerative colitis
UK	Urokinase
USCaP	Ultra-small size calcium phosphate
β-CD	β- cyclodextrin

8. Conflicts of interest

There are no conflicts to declare.

9. Acknowledgement

This work was supported by Australian National Health and Medical Research Council (HTT: APP1037310, APP1182347, APP2002827) and National Heart Foundation of Australia (HTT: 102761).

10. References

1. T. Morrow and L. H. Felcone, *Biotechnol Healthc*, 2004, **1**, 24-29.
2. J. C. N. Chan and A. T. C. Chan, *ESMO Open*, 2017, **2**, e000180.
3. in *Therapeutic Antibody Engineering*, eds. W. R. Strohl and L. M. Strohl, Woodhead Publishing, 2012, DOI: https://doi.org/10.1533/9781908818096.1, pp. 1-595.
4. S. Marqus, E. Pirogova and T. J. Piva, *Journal of Biomedical Science*, 2017, **24**, 21.
5. A. Mahipal and A. Grothey, *Journal of Oncology Practice*, 2016, **12**, 1219-1228.
6. V. Schirrmacher, *Int J Oncol*, 2019, **54**, 407-419.
7. J. S. Van Taunay, M. T. Albelda, J. C. Frias and M. J. Lipinski, *Journal of Cardiovascular Pharmacology*, 2018, **72**, 77-85.

8. M. Bliss, *Bull Hist Med*, 1982, **56**, 554-568.
9. U. S. F. a. D. Administration, *Journal*, 2021.
10. PRNewswire, Global Biologics Market Analysis Report 2022-2025 & 2030 Featuring Merck & Co, AbbVie, F. Hoffmann-La Roche, Johnson & Johnson, & Pfizer, https://www.prnewswire.com/news-releases/global-biologics-market-analysis-report-2022-2025--2030-featuring-merck--co-abbvie-f-hoffmann-la-roche-johnson--johnson--pfizer-301530433.html, (accessed 05.10, 2022).
11. S. W. Chung, T. A. Hil-lal and Y. Byun, *J Drug Target*, 2012, **20**, 481-501.
12. R. Bajracharya, J. G. Song, S. Y. Back and H.-K. Han, *Computational and Structural Biotechnology Journal*, 2019, **17**, 1290-1308.
13. B. Homayun, X. Lin and H.-J. Choi, *Pharmaceutics*, 2019, **11**, 129.
14. S. J. Won, X. N. Tang, S. W. Suh, M. A. Yenari and R. A. Swanson, *Ann Neurol*, 2011, **70**, 583-590.
15. Y. Jiang, J. Han, P. Spencer, Y. Li, S. J. Vodovoz, M.-M. Ning, N. Liu, X. Wang and A. S. Dumont, *Brain Hemorrhages*, 2021, **2**, 116-123.
16. H. Bardania, S. A. Shojaosadati, F. Kobarfard, F. Dorkoosh, M. E. Zadeh, M. Naraki and M. Faizi, *Journal of Thrombosis and Thrombolysis*, 2017, **43**, 184-193.
17. S. Gouda, R. George Kerry, G. Das and J. Kumar Patra, in *Nanomaterials in Plants, Algae and Microorganisms*, eds. D. K. Tripathi, P. Ahmad, S. Sharma, D. K. Chauhan and N. K. Dubey, Academic Press, 2019, DOI: https://doi.org/10.1016/B978-0-12-811488-9.00011-1, pp. 219-235.
18. S. Sim and N. K. Wong, *Biomed Rep*, 2021, **14**, 42-42.
19. M. J. Mitchell, M. M. Billingsley, R. M. Haley, M. E. Wechsler, N. A. Peppas and R. Langer, *Nature Reviews Drug Discovery*, 2021, **20**, 101-124.
20. J. K. Patra, Das, L. Fraceto, E. Campos, M. D. P. Rodríguez-Torres, L. Acosta-Torres, L. Diaz-Torres, R. Grillo, M. Swamy, S. Sharma, S. Habtemariam and H. Shin, *Journal of Nanobiotechnology*, 2018, **16**.
21. H. C. Huang, S. Barua, G. Sharma, S. K. Dey and K. Rege, *J Control Release*, 2011, **155**, 344-357.
22. R. Chakravarty, S. Goel, A. Dash and W. Cai, *Q J Nucl Med* 2017, **61**, 181-204.
23. H. Wang, R. Kumar, D. Nagesha, R. I. Duclos, S. Sridhar and S. J. Gatley, *Nuclear Medicine and Biology*, 2015, **42**, 65-70.
24. H. T. Ta, S. Prabhu, E. Leitner, F. Jia, D. von Elverfeldt, K. E. Jackson, T. Heidt, A. K. N. Nair, H. Pearce and C. Von Zur Muhlen, *Circulation Research*, 2011, **109**, 365-373.
25. H. T. Ta, Z. Li, C. E. Hagemeyer, G. Cowin, S. Zhang, J. Palasubramaniam, K. Alt, X. Wang, K. Peter and A. K. Whittaker, *Biomaterials*, 2017, **134**, 31-42.
26. H. T. Ta, N. Arndt, Y. Wu, H. J. Lim, S. Landeen, R. Zhang, D. Kamato, P. J. Little, A. K. Whittaker and Z. P. Xu, *Nanoscale*, 2018, **10**, 15103-15115.
27. H. T. Ta, Z. Li, Y. Wu, G. Cowin, S. Zhang, A. Yago, A. K. Whittaker and Z. P. Xu, *Materials Research Express*, 2017, **4**, 116105.
28. N. N. M. Yusof, A. McCann, P. J. Little and H. T. Ta, *Thrombosis research*, 2019, **177**, 161-171.
29. K. X. Vazquez-Prada, J. Lam, D. Kamato, Z. P. Xu, P. J. Little and H. T. Ta, *Arteriosclerosis, Thrombosis, and Vascular Biology*, 2021, **41**, 601-613.
30. Y. Liu, Y. Wu, R. Zhang, J. Lam, J. C. Ng, Z. P. Xu, L. Li and H. T. Ta, *ACS Applied Bio Materials*, 2019, **2**, 5930-5940.
31. N. Arndt, H. D. Tran, R. Zhang, Z. P. Xu and H. T. Ta, *Advanced Science*, 2020, **7**, 2001476.
32. Y. Wu, K. X. Vazquez-Prada, Y. Liu, A. K. Whittaker, R. Zhang and H. T. Ta, *Nanotheranostics*, 2021, **5**, 499.
33. H. Ta, S. Prabhu, E. Leitner, K. Putnam, F. Jia, N. Bassler, K. Peter and C. Hagemeyer, *Heart, Lung and Circulation*, 2010, **19**, S10.

34. A. U. Rehman, Y. Wu, H. D. Tran, K. Vazquez-Prada, Y. Liu, H. Adelnia, N. D. Kurniawan, M. N. Anjum, S. S. Moonshi and H. T. Ta, *ACS Applied Nano Materials*, 2021, **4**, 10136-10147.
35. S. S. Moonshi, Y. Wu and H. T. Ta, *Wiley Interdisciplinary Reviews: Nanomedicine and Nanobiotechnology*, 2022, **14**, e1760.
36. Y. Wu, Y. Yang, W. Zhao, Z. P. Xu, P. J. Little, A. K. Whittaker, R. Zhang and H. T. Ta, *Journal of Materials Chemistry B*, 2018, **6**, 4937-4951.
37. Y. Wu, R. Zhang, H. D. Tran, N. D. Kurniawan, S. S. Moonshi, A. K. Whittaker and H. T. Ta, *ACS Applied Nano Materials*, 2021, **4**, 3604-3618.
38. Y. Wu, G. Cowin, S. S. Moonshi, H. D. Tran, N. A. Fithri, A. K. Whittaker, R. Zhang and H. T. Ta, *Materials Science and Engineering: C*, 2021, **131**, 112477.
39. Z. Ferdous and A. Nemmar, *Int J Mol Sci*, 2020, **21**.
40. M. Fisichella, F. Berenguer, G. Steinmetz, M. Auffan, J. Rose and O. Prat, *BMC genomics*, 2014, **15**, 1-15.
41. S. Aalapati, S. Ganapathy, S. Manapuram, G. Anumolu and B. M. Prakya, *Nanotoxicology*, 2014, **8**, 786-798.
42. G. Yang, S. Z. F. Phua, A. K. Bindra and Y. Zhao, *Advanced Materials*, 2019, **31**, 1805730.
43. A. Akbarzadeh, R. Rezaei-Sadabady, S. Davaran, S. W. Joo, N. Zarghami, Y. Hanifehpour, M. Samiei, M. Kouhi and K. Nejati-Koshki, *Nanoscale Res Lett*, 2013, **8**, 102-102.
44. E. Beltrán-Gracia, A. López-Camacho, I. Higuera-Ciapara, J. B. Velázquez-Fernández and A. A. Vallejo-Cardona, *Cancer Nanotechnology*, 2019, **10**, 11.
45. M. Rahman, S. Beg, A. Verma, F. Anwar, A. Samad and V. Kumar, in *Nanotechnology-Based Approaches for Targeting and Delivery of Drugs and Genes*, eds. V. Mishra, P. Kesharwani, M. C. I. Mohd Amin and A. Iyer, Academic Press, 2017, DOI: https://doi.org/10.1016/B978-0-12-809717-5.00005-1, pp. 151-166.
46. L. Sercombe, T. Veerati, F. Moheimani, S. Y. Wu, A. K. Sood and S. Hua, *Front Pharmacol*, 2015, **6**, 286.
47. H. Idrees, S. Z. J. Zaidi, A. Sabir, R. U. Khan, X. Zhang and S.-U. Hassan, *Nanomaterials (Basel)*, 2020, **10**, 1970.
48. S. Agarwal, *Macromolecular Chemistry and Physics*, 2020, **221**, 2000017.
49. S. Biswas, P. P. Deshpande, G. Navarro, N. S. Dodwadkar and V. P. Torchilin, *Biomaterials*, 2013, **34**, 1289-1301.
50. A. Gagliardi, E. Giuliano, E. Venkateswararao, M. Fresta, S. Bulotta, V. Awasthi and D. Cosco, *Frontiers in pharmacology*, 2021, **12**, 601626-601626.
51. V. Fasiku, E. K. Amuhaya, K. M. Rajab and C. A. Omolo, in *Nano- and Microencapsulation - Techniques and Applications*, 2021, DOI: 10.5772/intechopen.93364.
52. Z. Zhou and M. Hartmann, *Topics in Catalysis*, 2012, **55**, 1081-1100.
53. S. A. Edwards and D. R. M. Williams, *Physical review letters*, 2004, **92**, 248303.
54. M. Boström, D. R. M. Williams and B. W. Ninham, *Physical review letters*, 2001, **87**, 168103.
55. H. H. Nguyen and M. Kim, *Applied Science and Convergence Technology*, 2017, **26**, 157-163.
56. S. Smith, K. Goodge, M. Delaney, A. Struzyk, N. Tansey and M. Frey, *Nanomaterials (Basel)*, 2020, **10**.
57. N. Hoshyar, S. Gray, H. Han and G. Bao, *Nanomedicine*, 2016, **11**, 673-692.
58. F. Szoka and D. Papahadjopoulos, *Proceedings of the national academy of sciences*, 1978, **75**, 4194-4198.
59. J. S. Suk, Q. Xu, N. Kim, J. Hanes and L. M. Ensign, *Adv Drug Deliv Rev*, 2016, **99**, 28-51.
60. S. J. Park, *Int J Nanomedicine*, 2020, **15**, 5783-5802.
61. S. L. Perry and D. J. McClements, *Molecules*, 2020, **25**, 1161.
62. S. Wang, P. Huang and X. Chen, *ACS Nano*, 2016, **10**, 2991-2994.

63. O. Martínez-Muñoz, L. Ospina-Giraldo and C.-E. Mora-Huertas, 2020, DOI: 10.5772/intechopen.93338.
64. J. T, *Journal of Nanomedicine & Nanotechnology*, 2016, **7**.
65. D. Panigrahi, P. K. Sahu, S. Swain and R. K. Verma, *SN Applied Sciences*, 2021, **3**, 638.
66. C. Chen, W. Liu, P. Jiang and T. Hong, *Micromachines (Basel)*, 2019, **10**, 125.
67. B. K. Sabjan, M. S. Munawar, D. Rajendiran, K. S. Vinoji and K. Kasinathan, *Current Drug Research Reviews*, 2020, **12**, 4-15.
68. D. Essa, P. P. D. Kondiah, Y. E. Choonara and V. Pillay, *Frontiers in Bioengineering and Biotechnology*, 2020, **8**.
69. M. Zamanlu, M. Eskandani, J. Barar, M. Jaymand, P. S. Pakchin and M. Farhoudi, *Journal of Drug Delivery Science and Technology*, 2019, **53**, 101165.
70. Y. Dölen, U. Gileadi, J. L. Chen, M. Valente, J. H. A. Creemers, E. A. W. Van Dinther, N. K. van Riessen, E. Jäger, M. Hruby, V. Cerundolo, M. Diken, C. G. Figdor and I. J. M. de Vries, *Front Immunol*, 2021, **12**, 641703.
71. J. H. A. Creemers, I. Pawlitzky, K. Grosios, U. Gileadi, M. R. Middleton, W. R. Gerritsen, N. Mehra, L. Rivoltini, I. Walters, C. G. Figdor, P. B. Ottevanger and I. J. M. de Vries, *BMJ Open*, 2021, **11**, e050725.
72. Q.-P. Feng, Y.-T. Zhu, Y.-Z. Yuan, W.-J. Li, H.-H. Yu, M.-Y. Hu, S.-Y. Xiang and S.-Q. Yu, *Materials Science and Engineering: C*, 2021, **124**, 112039.
73. M. Iqbal, N. Zafar, H. Fessi and A. Elaissari, *International Journal of Pharmaceutics*, 2015, **496**, 173-190.
74. J. D. Ospina-Villa, C. Gómez-Hoyos, R. Zuluaga-Gallego and O. Triana-Chávez, *Journal of Microbiological Methods*, 2019, **162**, 1-7.
75. S. Matsumoto, T. Inoue, M. Kohda and K. Ikura, *Journal of Colloid and Interface Science*, 1980, **77**, 555-563.
76. Y. F. Maa and C. C. Hsu, *Pharm Dev Technol*, 1999, **4**, 233-240.
77. J. Cai, X. Huai, S. Liang and X. Li, *Frontiers of Energy and Power Engineering in China*, 2010, **4**, 313-318.
78. E. Steiert, L. Radi, M. Fach and P. R. Wich, *Macromolecular Rapid Communications*, 2018, **39**, 1800186.
79. M. Boushra, S. Tous, G. Fetih, H.-Y. Xue and H.-L. Wong, *Journal of Drug Delivery Science and Technology*, 2019, **49**, 632-641.
80. D. L. Priwitaningrum, J. Jentsch, R. Bansal, S. Rahimian, G. Storm, W. E. Hennink and J. Prakash, *International Journal of Pharmaceutics*, 2020, **585**, 119535.
81. B. Xiao, Z. Xu, E. Viennois, Y. Zhang, Z. Zhang, M. Zhang, M. K. Han, Y. Kang and D. Merlin, *Molecular Therapy*, 2017, **25**, 1628-1640.
82. H. Laroui, G. Dalmasso, H. T. T. Nguyen, Y. Yan, S. V. Sitaraman and D. Merlin, *Gastroenterology*, 2010, **138**, 843-853.
83. F. Minooei, J. R. Fried, J. L. Fuqua, K. E. Palmer and J. M. Steinbach-Rankins, *Journal*, 2021, **16**, 1189-1206.
84. X. Li, A. n. Sun, Y.-j. Liu, W.-j. Zhang, N. Pang, S.-x. Cheng and X.-r. Qi, *NPG Asia Materials*, 2018, **10**, 238-254.
85. Z. Zhang, Y. Heng, W. Cheng, Y. Pan, S. Ni and H. Li, *Materials & Design*, 2021, **204**, 109648.
86. L. C. Lin, C. Y. Huang, B. Y. Yao, J. C. Lin, A. Agrawal, A. Algaissi, B. H. Peng, Y. H. Liu, P. H. Huang, R. H. Juang, Y. C. Chang, C. T. Tseng, H. W. Chen and C. J. Hu, *Adv Funct Mater*, 2019, **29**, 1807616.
87. M. S. Ural, M. Menéndez-Miranda, G. Salzano, J. Mathurin, E. N. Aybeke, A. Deniset-Besseau, A. Dazzi, M. Porcino, C. Martineau-Corcos and R. Gref, *Pharmaceutics*, 2021, **13**, 1992.
88. R. Liao, J. Pon, M. Chungyoun and E. Nance, *Biomaterials*, 2020, **257**, 120238.
89. T. L. Freitag, J. R. Podojil, R. M. Pearson, F. J. Fokta, C. Sahl, M. Messing, L. C.

Andersson, K. Leskinen, P. Saavalainen, L. I. Hoover, K. Huang, D. Phippard, S. Maleki, N. J. C. King, L. D. Shea, S. D. Miller, S. K. Meri and D. R. Getts, *Gastroenterology*, 2020, **158**, 1667-1681.e1612.
90. J. Su and A. Cavaco-Paulo, *Ultrason Sonochem*, 2021, **76**, 105653-105653.
91. N. Leister and H. Karbstein, *Colloids and Interfaces*, 2020, **4**, 8.
92. M. M. Rahman, B. Byanju, D. Grewell and B. P. Lamsal, *Ultrason Sonochem*, 2020, **64**, 105019.
93. H. Fessi, F. Puisieux, J. P. Devissaguet, N. Ammoury and S. Benita, *International Journal of Pharmaceutics*, 1989, **55**, R1-R4.
94. A. Arizaga, G. Ibarz, R. Piñol and A. Urtizberea, *Journal of Experimental Nanoscience*, 2014, **9**, 561-569.
95. J. Tao, S. F. Chow and Y. Zheng, 2018.
96. R. Rietscher, C. Thum, C.-M. Lehr and M. Schneider, *Pharmaceutical Research*, 2015, **32**, 1859-1863.
97. J. Hiemer, A. Clausing, T. Schwarz and K. Stöwe, *Chemical Engineering & Technology*, 2019, **42**, 2018-2027.
98. M. Morales-Cruz, G. M. Flores-Fernández, M. Morales-Cruz, E. A. Orellano, J. A. Rodriguez-Martinez, M. Ruiz and K. Griebenow, *Results in Pharma Sciences*, 2012, **2**, 79-85.
99. L. C. Nelemans, M. Buzgo and A. Simaite, *Proceedings*, 2021, **78**.
100. J. L. C. De Queiroz, R. O. De Araújo Costa, L. L. Rodrigues Matias, A. F. De Medeiros, A. F. Teixeira Gomes, T. D. Santos Pais, T. S. Passos, B. L. L. Maciel, E. A. Dos Santos and A. H. De Araújo Morais, *Food Hydrocolloids*, 2018, **84**, 247-256.
101. Y. Liu, G. Yang, D. Zou, Y. Hui, K. Nigam, A. P. J. Middelberg and C.-X. Zhao, *Industrial & Engineering Chemistry Research*, 2020, **59**, 4134-4149.
102. C. E. Markwalter and R. K. Prud'homme, *J Pharm Sci*, 2018, **107**, 2465-2471.
103. R. F. Pagels and R. K. Prud'homme, *Journal of Controlled Release*, 2015, **219**, 519-535.
104. K. M. Pustulka, A. R. Wohl, H. S. Lee, A. R. Michel, J. Han, T. R. Hoye, A. V. McCormick, J. Panyam and C. W. Macosko, *Molecular Pharmaceutics*, 2013, **10**, 4367-4377.
105. Y. Liu, C. Cheng, R. K. Prud’homme and R. O. Fox, *Chemical Engineering Science*, 2008, **63**, 2829-2842.
106. S. L. Levit, R. C. Walker and C. Tang, *Polymers*, 2019, **11**.
107. C. E. Markwalter, R. F. Pagels, A. N. Hejazi, A. G. R. Gordon, A. L. Thompson and R. K. Prud’homme, *The AAPS Journal*, 2020, **22**, 18.
108. H. Adelnia, H. D. Tran, P. J. Little, I. Blakey and H. T. Ta, *ACS Biomaterials Science & Engineering*, 2021, **7**, 2083-2105.
109. Z. Zeng, C. Dong, P. Zhao, Z. Liu, L. Liu, H.-Q. Mao, K. W. Leong, X. Gao and Y. Chen, *Advanced Healthcare Materials*, 2019, **8**, 1801010.
110. S. McManus, Y. Zhang, B. Kim, B. Lee, M. ElSayed and R. Prud'homme, *Precision Nanomedicine*, 2020, DOI: 10.33218/001c.18519.
111. S. Liu, S. de Beer, K. M. Batenburg, H. Gojzewski, J. Duvigneau and G. J. Vancso, *ACS Applied Materials & Interfaces*, 2021, **13**, 17034-17045.
112. A. C. Mendes, E. T. Baran, R. L. Reis and H. S. Azevedo, *Wiley Interdisciplinary Reviews: Nanomedicine and Nanobiotechnology*, 2013, **5**, 582-612.
113. J. Gu, X. Chen, X. Fang and X. Sha, *Acta Biomaterialia*, 2017, **57**, 156-169.
114. S. C. Larnaudie, J. C. Brendel, K. A. Jolliffe and S. Perrier, *ACS Macro Letters*, 2017, **6**, 1347-1351.
115. M. S. Lee, N. W. Kim, J. E. Lee, M. G. Kim, Y. Yin, S. Y. Kim, B. S. Ko, A. Kim, J. H. Lee, S. Y. Lim, D. W. Lim, S. H. Kim, J. W. Park, Y. T. Lim and J. H. Jeong, *Acta Biomaterialia*, 2018, **81**, 231-241.
116. O. H. Orasan, G. Ciulei, A. Cozma, M. Sava and D. L. Dumitrascu, *Clujul Med*, 2016, **89**, 24-31.

117. M. Gudowska, E. Gruszewska, A. Panasiuk, B. Cylwik, R. Flisiak, M. Świderska, M. Szmitkowski and L. Chrostek, *Clin Exp Med*, 2016, **16**, 523-528.
118. R. E. Avila, R. A. Carmo, P. Farah Kde, A. L. Teixeira, L. V. Coimbra, C. M. Antunes and J. R. Lambertucci, *Braz J Infect Dis*, 2010, **14**, 335-341.
119. D. C. Rockey and D. M. Bissell, *Hepatology*, 2006, **43**, S113-120.
120. J. F. Hansen, K. M. Christiansen, B. Staugaard, B. K. Moessner, S. Lillevang, A. Krag and P. B. Christensen, *PLOS ONE*, 2019, **14**, e0212036.
121. T. Mei, A. Kim, L. B. Vong, A. Marushima, S. Puentes, Y. Matsumaru, A. Matsumura and Y. Nagasaki, *Biomaterials*, 2019, **215**, 119209.
122. H. Zhang, Y. Pei, L. Gao, Q. He, H. Zhang, L. Zhu, Z. Zhang and L. Hou, *Nano Today*, 2021, **38**, 101186.
123. Q. Ma, L. Bian, X. Zhao, X. Tian, H. Yin, Y. Wang, A. Shi and J. Wu, *Mater Today Bio*, 2022, **13**, 100181.
124. B. J. Wall, M. F. Will, G. K. Yawson, P. J. Bothwell, D. C. Platt, C. F. Apuzzo, M. A. Jones, G. M. Ferrence and M. I. Webb, *J Med Chem*, 2021, **64**, 10124-10138.
125. S. B. Alvi, S. Ahmed, D. Sridharan, Z. Naseer, N. Pracha, H. Wang, K. D. Boudoulas, W. Zhu, N. Sayed and M. Khan, *Front Cardiovasc Med*, 2021, **8**, 742315.
126. Z. Jin, Y. Zhao, Y. Sun, B. Zhang, H. Wang, Y. Wu, Y. Zhu, C. Zhu, T. Hu and X. Du, *Nature structural & molecular biology*, 2020, **27**, 529-532.
127. W. Yan, Y. Zheng, X. Zeng, B. He and W. Cheng, *Signal Transduction and Targeted Therapy*, 2022, **7**, 26.
128. D. Giovinazzo, B. Bursac, I. Sbodio Juan, S. Nalluru, T. Vignane, M. Snowman Adele, M. Albacarys Lauren, W. Sedlak Thomas, R. Torregrossa, M. Whiteman, R. Filipovic Milos, H. Snyder Solomon and D. Paul Bindu, *Proceedings of the National Academy of Sciences*, 2021, **118**, e2017225118.
129. M. S. Bahniuk, A. K. Alshememry, S. V. Elgersma and L. D. Unsworth, *Journal of Nanobiotechnology*, 2018, **16**, 15.
130. H. Cheng, X. Zhang, L. Qin, Y. Huo, Z. Cui, C. Liu, Y. Sun, J. Guan and S. Mao, *Journal of Controlled Release*, 2020, **321**, 641-653.
131. H. F. Moffett, M. E. Coon, S. Radtke, S. B. Stephan, L. McKnight, A. Lambert, B. L. Stoddard, H. P. Kiem and M. T. Stephan, *Nat Commun*, 2017, **8**, 389.
132. T. T. Smith, S. B. Stephan, H. F. Moffett, L. E. McKnight, W. Ji, D. Reiman, E. Bonagofski, M. E. Wohlfahrt, S. P. S. Pillai and M. T. Stephan, *Nature Nanotechnology*, 2017, **12**, 813-820.
133. J. Karlsson, Y. Rui, K. L. Kozielski, A. L. Placone, O. Choi, S. Y. Tzeng, J. Kim, J. J. Keyes, M. I. Bogorad, K. Gabrielson, H. Guerrero-Cazares, A. Quiñones-Hinojosa, P. C. Searson and J. J. Green, *Nanoscale*, 2019, **11**, 20045-20057.
134. H. J. Kim, S. Ogura, T. Otabe, R. Kamegawa, M. Sato, K. Kataoka and K. Miyata, *ACS Central Science*, 2019, **5**, 1866-1875.
135. S. Abbasi, S. Uchida, K. Toh, T. A. Tockary, A. Dirisala, K. Hayashi, S. Fukushima and K. Kataoka, *Journal of Controlled Release*, 2021, **332**, 260-268.
136. L. Y. Chan, Y. L. Khung and C.-Y. Lin, *Journal*, 2019, **9**.
137. A. J. Atkinson, Jr., *Transl Clin Pharmacol*, 2017, **25**, 117-124.
138. J. Liang, C. Wu, X. Zhou, Y. Shi, J. Xu, X. Cai, T. Fu, D. Ma and W. Xue, *Colloids and Surfaces B: Biointerfaces*, 2021, **205**, 111918.
139. R. K. Dhandapani, D. Gurusamy and S. R. Palli, *ACS Applied Bio Materials*, 2021, **4**, 4310-4318.
140. P.-F. Cui, L.-Y. Qi, Y. Wang, R.-Y. Yu, Y.-J. He, L. Xing and H.-L. Jiang, *Journal of Controlled Release*, 2019, **303**, 253-262.
141. M.-A. Nguyen, H. Wyatt, L. Susser, M. Geoffrion, A. Rasheed, A.-C. Duchez, M. L. Cottee, E. Afolayan, E. Farah, Z. Kahiel, M. Côté, S. Gadde and K. J. Rayner, *ACS Nano*, 2019, **13**, 6491-6505.

142. T. T. Smith, S. B. Stephan, H. F. Moffett, L. E. McKnight, W. Ji, D. Reiman, E. Bonagofski, M. E. Wohlfahrt, S. P. S. Pillai and M. T. Stephan, *Nat Nanotechnol*, 2017, **12**, 813-820.
143. S. Bastaki, S. Aravindhan, N. Ahmadpour Saheb, M. Afsari Kashani, A. Evgenievich Dorofeev, F. Karoon Kiani, H. Jahandideh, F. Beigi Dargani, M. Aksoun, A. Nikkhoo, A. Masjedi, A. Mahmoodpoor, M. Ahmadi, S. Dolati, S. Namvar Aghdash and F. Jadidi-Niaragh, *Life Sciences*, 2021, **266**, 118847.
144. I. Bu, Y.-S. Fu, J.-F. Li and T.-F. Guo, *RSC Adv.*, 2017, **7**, 46651-46656.
145. L. Peltonen, H. Valo, R. Kolakovic, T. Laaksonen and J. Hirvonen, *Expert Opin Drug Deliv*, 2010, **7**, 705-719.
146. J. A. Bhushani and C. Anandharamakrishnan, *Trends in Food Science & Technology*, 2014, **38**, 21-33.
147. Y. Liu, X. Chen, Y. Gao, D.-G. Yu and P. Liu, *Journal of Nanobiotechnology*, 2022, **20**, 244.
148. W. Jiang, X. Zhang, P. Liu, Y. Zhang, W. Song, D.-G. Yu and X. Lu, *Advanced Composites and Hybrid Materials*, 2022, **5**, 3045-3056.
149. X. Liu, M. Zhang, W. Song, Y. Zhang, D.-G. Yu and Y. Liu, *Journal*, 2022, **8**.
150. P. Mishra, P. Gupta and V. Pruthi, *Materials Science and Engineering: C*, 2021, **119**, 111450.
151. D. Han, S. Sherman, S. Filocamo and A. J. Steckl, *Acta Biomaterialia*, 2017, **53**, 242-249.
152. M. Zamani, M. P. Prabhakaran, E. S. Thian and S. Ramakrishna, *International Journal of Pharmaceutics*, 2014, **473**, 134-143.
153. N. Yaghoobi, R. Faridi Majidi, M. A. Faramarzi, H. Baharifar and A. Amani, *Adv Pharm Bull*, 2017, **7**, 131-139.
154. A. Hasanpour, F. Esmaeili, H. Hosseini and A. Amani, *Materials Science and Engineering: C*, 2021, **118**, 111427.
155. F. Bensebaa, in *Interface Science and Technology*, ed. F. Bensebaa, Elsevier, 2013, vol. 19, pp. 85-146.
156. G. Lüttgens and N. Wilson, in *Electrostatic Hazards*, eds. G. Lüttgens and N. Wilson, Butterworth-Heinemann, Oxford, 1997, DOI: https://doi.org/10.1016/B978-075062782-5/50003-7, pp. 14-38.
157. T. Si, L. Zhang, G. Li, C. J. Roberts, X. Yin and R. Xu, *J Biomed Opt*, 2013, **18**, 075003.
158. L. Yu, Q. Sun, Y. Hui, A. Seth, N. Petrovsky and C.-X. Zhao, *Journal of Colloid and Interface Science*, 2019, **539**, 497-503.
159. J. Pessi, H. A. Santos, I. Miroshnyk, JoukoYliruusi, D. A. Weitz and S. Mirza, *International Journal of Pharmaceutics*, 2014, **472**, 82-87.
160. O. F. Khan, P. S. Kowalski, J. C. Doloff, J. K. Tsosie, V. Bakthavatchalu, C. B. Winn, J. Haupt, M. Jamiel, R. Langer and D. G. Anderson, *Science Advances*, 2018, **4**, eaar8409.
161. S. Gimondi, C. F. Guimarães, S. F. Vieira, V. M. F. Gonçalves, M. E. Tiritan, R. L. Reis, H. Ferreira and N. M. Neves, *Nanomedicine: Nanotechnology, Biology and Medicine*, 2022, **40**, 102482.
162. Y. Qiu, Y. Liu, Y. Xu, Z. Li and J. Chen, *ELECTROPHORESIS*, 2020, **41**, 902-908.
163. G.-Y. Ahn, I. Choi, M. Song, S. K. Han, K. Choi, Y.-H. Ryu, D.-H. Oh, H.-W. Kang and S.-W. Choi, *ACS Macro Letters*, 2022, **11**, 127-134.
164. X. Yang, Z. Pan, M. R. Choudhury, Z. Yuan, A. Anifowose, B. Yu, W. Wang and B. Wang, *Medicinal Research Reviews*, 2020, **40**, 2682-2713.
165. V. Agrahari, V. Agrahari and A. K. Mitra, *Ther Deliv*, 2016, **7**, 257-278.
166. B. S. Zolnik and D. J. Burgess, *Journal of Controlled Release*, 2007, **122**, 338-344.
167. M. A. Tracy, K. L. Ward, L. Firouzabadian, Y. Wang, N. Dong, R. Qian and Y. Zhang, *Biomaterials*, 1999, **20**, 1057-1062.
168. C. E. Holy, S. M. Dang, J. E. Davies and M. S. Shoichet, *Biomaterials*, 1999, **20**, 1177-1185.
169. M. Shameem, H. Lee and P. P. DeLuca, *Aaps Pharmsci*, 1999, **1**, 1-6.

170. S. A. Sufi, M. Hoda, S. Pajaniradje, V. Mukherjee, S. M. Coumar and R. Rajagopalan, *International Journal of Pharmaceutics*, 2020, **588**, 119738.
171. F. Canfarotta, A. Poma, A. Guerreiro and S. Piletsky, *Nat Protoc*, 2016, **11**, 443-455.
172. A. Motaharian, M. R. M. Hosseini and K. Naseri, *Sensors and Actuators B: Chemical*, 2019, **288**, 356-362.
173. X. Wang, Y. Pei, Y. Hou and Z. Pei, *Polymers*, 2019, **11**, 313.
174. X. Zhang, D. An, R. Zhang, Y. Huang and Z. Liu, *International Journal of Pharmaceutics*, 2022, **615**, 121476.
175. D. Yin, X. Li, Y. Ma and Z. Liu, *Chemical Communications* 2017, **53**.
176. H. R. Culver and N. A. Peppas, *Chem Mater*, 2017, **29**, 5753-5761.
177. R. Fekety, *Medical Clinics of North America*, 1982, **66**, 175-181.
178. H. Su, C. A. Hurd Price, L. Jing, Q. Tian, J. Liu and K. Qian, *Materials Today Bio*, 2019, **4**, 100033.
179. K. Kim, J. Guo, Z. Liang and D. Fan, *Advanced Functional Materials*, 2018, **28**, 1705867.
180. H. Liu, H. Wang, X. Lu, V. Murugadoss, M. Huang, H. Yang, F. Wan, D.-G. Yu and Z. Guo, *Advanced Composites and Hybrid Materials*, 2022, **5**, 1017-1029.
181. L. Liu, W. Yao, X. Xie, J. Gao and X. Lu, *Journal of Nanobiotechnology*, 2021, **19**, 235.
182. M. Wang, D.-G. Yu, G. R. Williams and S. W. Bligh, *Journal*, 2022, **14**.
183. L. R. Baden, H. M. El Sahly, B. Essink, K. Kotloff, S. Frey, R. Novak, D. Diemert, S. A. Spector, N. Rouphael, C. B. Creech, J. McGettigan, S. Khetan, N. Segall, J. Solis, A. Brosz, C. Fierro, H. Schwartz, K. Neuzil, L. Corey, P. Gilbert, H. Janes, D. Follmann, M. Marovich, J. Mascola, L. Polakowski, J. Ledgerwood, B. S. Graham, H. Bennett, R. Pajon, C. Knightly, B. Leav, W. Deng, H. Zhou, S. Han, M. Ivarsson, J. Miller and T. Zaks, *N Engl J Med*, 2021, **384**, 403-416.
184. F. P. Polack, S. J. Thomas, N. Kitchin, J. Absalon, A. Gurtman, S. Lockhart, J. L. Perez, G. Pérez Marc, E. D. Moreira, C. Zerbini, R. Bailey, K. A. Swanson, S. Roychoudhury, K. Koury, P. Li, W. V. Kalina, D. Cooper, R. W. Frenck, Jr., L. L. Hammitt, Ö. Türeci, H. Nell, A. Schaefer, S. Ünal, D. B. Tresnan, S. Mather, P. R. Dormitzer, U. Şahin, K. U. Jansen and W. C. Gruber, *N Engl J Med*, 2020, **383**, 2603-2615.
185. S. J. Thomas, E. D. Moreira, Jr., N. Kitchin, J. Absalon, A. Gurtman, S. Lockhart, J. L. Perez, G. Pérez Marc, F. P. Polack, C. Zerbini, R. Bailey, K. A. Swanson, X. Xu, S. Roychoudhury, K. Koury, S. Bouguermouh, W. V. Kalina, D. Cooper, R. W. Frenck, Jr., L. L. Hammitt, Ö. Türeci, H. Nell, A. Schaefer, S. Ünal, Q. Yang, P. Liberator, D. B. Tresnan, S. Mather, P. R. Dormitzer, U. Şahin, W. C. Gruber and K. U. Jansen, *N Engl J Med*, 2021, **385**, 1761-1773.
186. P. T. Heath, E. P. Galiza, D. N. Baxter, M. Boffito, D. Browne, F. Burns, D. R. Chadwick, R. Clark, C. Cosgrove and J. Galloway, *New England Journal of Medicine*, 2021, **385**, 1172-1183.